Received February 28, 2021, accepted May 7, 2021, date of publication May 14, 2021, date of current version May 24, 2021.

Digital Object Identifier 10.1109/ACCESS.2021.3080326

Millimeter-Wave Spectrum Utilization Improvement in Multi-Operator Networks: A Framework Using the Equal Likelihood Criterion

RONY KUMER SAHA
Radio and Spectrum Laboratory, KDDI Research, Inc., Fujimino 356-8502, Japan
e-mail: ro-saha@kddi-research.jp

ABSTRACT In this paper, we present a framework to give a comprehensive review of how to improve the spectrum utilization of millimeter-wave (mmWave) systems using indoor small cells in multi-operator network scenarios. More specifically, the framework concerns with the improvement of the utilization of the 28 GHz mmWave spectrum allocated to an arbitrary number of mobile network operators (MNOs) in a country using numerous spectrum allocation techniques, namely Static and Equal Spectrum Allocation (SESA), Flexible and Unequal Spectrum Allocation (FUSA), and Countrywide Full Spectrum Allocation (CFSA). A number of spectrum utilization improvement mechanisms such as spectrum trading, spectrum sharing, and spectrum reusing are then exploited into SESA, FUSA, and CFSA techniques in four major-interconnected domains, including time, frequency, power, and space. Using the Equal Likelihood Criterion and the properties of left-justified Pascal's triangle, the average capacity, spectral efficiency (SE), and energy efficiency (EE) performance metrics for each spectrum allocation technique in each domain are derived. Extensive system-level numerical and simulation results and analyses are carried out to evaluate the performance of each technique in each domain for example scenario of a country with four MNOs. Overall, it is shown that, in the power-domain, CFSA outperforms SESA and FUSA (when operating either at the interweave or at the underlay spectrum access technique), whereas, in the time-domain and frequency-domain, SESA and FUSA outperform CFSA, in terms of the average capacity, SE, and EE. Finally, we show that CFSA in the power-domain outperforms SESA and FUSA operating in any domain to achieve the prospective SE and EE requirements for the sixth-generation (6G) mobile networks.

INDEX TERMS Spectrum utilization, multi-operator, millimeter-wave, 6G, mobile network, small cell, framework, equal likelihood, 28 GHz.

I. INTRODUCTION

A. BACKGROUND

The demand for high network capacity and user data rate is ever-increasing from one generation to another in mobile communication networks. For example, the sixth-generation (6G) mobile network is expected to be further upgraded and expanded from its predecessor the fifth-generation (5G) network to achieve 10 to 100 times higher data rate, system capacity, spectrum efficiency, and energy efficiency [1]. According to Shannon's capacity formula, the achievable capacity is directly proportional to the available radio spectrum bandwidth. However, the radio spectrum allocated to a Mobile Network Operator (MNO) is limited and expensive. Due to this reason, the traditional approaches to increasing the capacity by aggregating spectrum bandwidths of a number of bands (Fig.1) is no more considered sufficient.

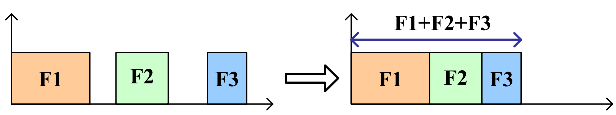

FIGURE 1. Spectrum aggregation (noncontiguous) [4].

So, addressing the high capacity and data rate demands with a limited spectrum bandwidth allocated to an MNO has become a major issue for the existing and upcoming 5G and beyond mobile networks. Since the radio spectrum is a natural

The associate editor coordinating the review of this manuscript and approving it for publication was Amjad Mehmood.

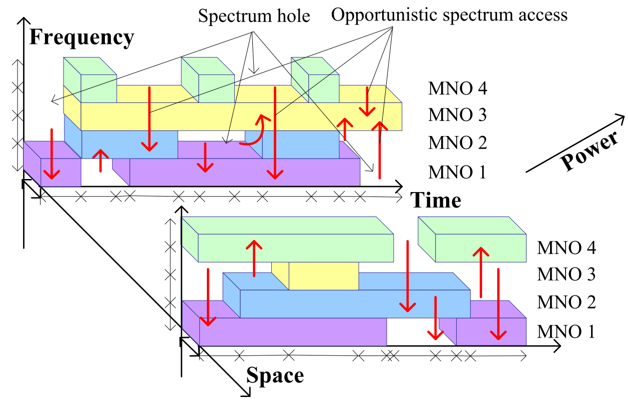

FIGURE 2. An example spectrum usage case of four MNOs in a country [4].

resource and cannot be increased on-demand, a potential approach to increasing the network capacity is to improve the utilization of the available radio spectrum allocated to each MNO in a country. This causes the spectrum utilization metric to become one of the key design approaches to address the ever-increasing network capacity and user data rate demands of existing and upcoming mobile networks.

Besides, techniques to allocate the spectrum to MNOs in a country play a considerable role in the efficient utilization of the allocated spectrum [2]. Further, spectrum utilization can be improved by exploiting numerous domains, namely time-domain (TD), frequency-domain (FD), power-domain (PD), and space-domain (SD), since the requirements to serve user traffic of different MNOs vary differently in radio resources (including time, frequency, and transmission power) and physical spaces as shown in Fig.2. Accordingly, a great portion of the allocated spectrum to an MNO may be left unused (shown as spectrum holes in Fig.2) in time, frequency, power, and space domains [3], [4]. This causes one MNO to be suffered from the scarcity of the required spectrum, whereas the other MNO to have an excessive amount of spectrum, for example, at any time in a given area.

Several mechanisms have already been proposed (e.g., spectrum trading, spectrum sharing, and spectrum reusing) in the existing literature to improve the utilization of the allocated spectrum to an MNO by exploiting further in TD, FD, PD, and SD. In spectrum sharing, the same spectrum can be shared among multiple MNOs subject to avoiding co-channel interference (CCI) in either TD, FD, or PD. In spectrum trading, an MNO with a shortage of allocated spectrum can lease spectrum from other MNOs in FD, each having unused or under-utilized spectra, in the secondary-level. In spectrum reusing, the same spectrum of an MNO can be reused in space subject to satisfying a certain CCI constraint in SD.

B. PROBLEM STATEMENT

The licensed spectrum in a country can be allocated primarily to its MNOs in a number of ways, namely, Static and Equal Spectrum Allocation (SESA) [5], Flexible and Unequal Spectrum Allocation (FUSA) [6], and Countrywide Full Spectrum Allocation (CFSA) [5], [7]. An equal amount of spectrum in SESA, whereas an unequal amount of spectrum in FUSA, is allocated to each MNO in a country. In contrast, in CFSA, each MNO in a country can get access to the countrywide full spectrum subject to avoiding the generated CCI due to operating at the same spectrum by all MNOs. In this regard, all spectrum utilization improvement mechanisms cannot be applied to each spectrum allocation technique. Rather, depending on how the spectrum is allocated to MNOs in SESA, FUSA, and CFSA techniques, an improvement mechanism can be applied. For example, spectrum sharing can be applied to all techniques, whereas spectrum trading can be applied to only SESA to balance the countrywide full spectrum distribution among MNOs in the secondary-level. However, like spectrum sharing, spectrum reusing can be applicable to all techniques.

Besides, the performance of a spectrum allocation technique differs from the other, and the impact of exploiting any spectrum utilization improvement mechanism in one domain is different from another. Since the improvement in spectrum utilization is a function of both the spectrum allocation technique, as well as the domain (i.e., TD, FD, or PD) exploited in the applicable spectrum improvement mechanism, a comprehensive and rigorous study on the performance of the combinations of a spectrum allocation technique and a domain exploited in the spectrum improvement mechanism is inevitable. However, to the best view of the authors, such a study is non-obvious, which can help select a suitable combination of a spectrum allocation technique and the corresponding domain to exploit the spectrum utilization improvement mechanisms to achieve the maximum utilization of the available spectrum for 5G and beyond mobile networks.

C. RELATED STUDY

Numerous researches [2], [8]–[10] have already addressed spectrum allocation problems in the existing literature. The authors in [2], [8] have addressed the spectrum allocation problems in cognitive radio systems, whereas the authors in [9] have addressed a dynamic frequency allocation scheme in heterogeneous networks. Further, the authors in [10] have presented a dynamic spectrum allocation algorithm to address channel conflict in vehicle networks. Furthermore, for SESA, the authors have considered SESA to present an underlay cognitive radio access technique in [11], whereas an interweave shared-use model in [12], to share the millimeter-wave (mmWave) spectrum of one MNO with another. For FUSA, the authors in [13] have presented the FUSA technique to allocate the mmWave spectrum to MNOs in a country to gain high spectrum utilization. Likewise, in [14], the authors have presented a spectrum utilization improvement technique for FUSA.

Besides, for CFSA, the authors have presented the idea of CFSA to overcome the constraints of SESA in [15]. The authors have detailed and evaluated the idea of CFSA in [7] for the allocation of the 28 GHz spectrum to all MNOs in a country. Moreover, in [5], CFSA has been emphasized as a key technique to improve spectrum utilization. In [16], a countrywide mmWave spectrum allocation and reuse technique has been proposed in a multi-operator scenario to allocate and reuse the mmWave spectrum to small cells deployed in multistory buildings. Besides, authors in [5] have defined main concerns and discussed solutions along with evaluating the performances of SESA, FUSA, and CFSA for the mmWave spectra operating at the indoor small cells. Moreover, recently, in [14], the authors have proposed two approaches to improve the mmWave spectrum utilization, one for SESA and the other for FUSA, in a multi-operator scenario.

Likewise, many research studies have already addressed spectrum utilization improvement mechanisms. More specifically, for spectrum sharing, the authors have studied the mmWave spectrum sharing approaches in [17], whereas the authors in [18] presented a hybrid mmWave spectrum access scheme. Further, the authors in [19], [20] have addressed dynamic spectrum sharing problems in multi-operator environments. Regarding spectrum trading, the authors in [21] proposed a dynamic exclusive-use spectrum access (DESA) method to improve the licensed mmWave spectrum utilization of all MNOs of a country by exploiting the secondary spectrum trading. Also, in [6], the authors have exploited mmWave spectrum trading in countrywide mobile network operators to improve spectral and energy efficiencies. the authors in [22] have presented a matching-based double action mechanism, whereas in [23], the authors have presented a bandwidth-auction game. Moreover, the authors in [24] have proposed a spectrum trading scheme using Evolutionary game theory, and the authors in [25] have formulated spectrum trading problems using contact theory. Similarly, for spectrum reusing, numerous fractional frequency reuse techniques have been addressed in [26]–[28]. Further, analytical models to reuse spectrum to indoor small cells have been presented in [29] for the microwave spectrum and in [30] for the mmWave spectrum. Furthermore, the authors in [7], [16] have presented reusing the 28 GHz mmWave spectrum to indoor small cells.

Moreover, numerous studies have addressed multiple domains to exploit the above spectrum utilization improvement mechanisms. Particularly, in TD, the authors have exploited TD almost blank subframe (ABS) based enhanced intercell interference coordination (eICIC) technique to avoid CCI between satellite users and small cell users in multistory buildings in [31] for satellite-mobile networks and in [32] for ultra-dense mobile networks. Moreover, the TD CCI avoidance scheme has been presented in [33] to derive the optimal amount of time for each MNO to operate at the countrywide full mmWave spectrum. Further, in FD, the authors in [13] have proposed a technique by exploiting the FD to define the amount of the mmWave spectrum to be allocated to an MNO corresponding to its number of subscribers at any spectrum license renewal term. Likewise, in [17], the authors have presented an FD CCI avoidance strategy to define the optimal amount of the mmWave spectrum for any indoor small cell of an MNO at any transmission time interval (TTI) in accordance with the density of small cell UEs of interferer MNOs within the coverage of the small cell.

Furthermore, in PD, by exploiting the PD to control the transmission power of indoor small cells of MNOs in a country, the authors have presented a technique employing the interweave spectrum access in [13], the underlay spectrum access in [11], and the hybrid interweave-underlay spectrum access in [34] to manage CCI and to share mmWave spectrum of one MNO with small cells of another MNO to improve the countrywide mmWave spectrum utilization. Moreover, in SD, the authors have exploited the SD within multistory buildings deployed with small cells of MNOs to reuse the allocated microwave spectrum in [29] and mmWave spectrum in [16], [30] to its indoor small cells more than once subject to satisfying a minimum interference limit set in prior by the MNO between co-channel small cells. Finally, in [35], the authors have exploited all four domains (i.e., TD, FD, PD, and SD) to present a theoretical framework, which has been detailed further in [36], for indoor small cells to achieve the prospective SE and EE requirements for 6G mobile networks.

D. CONTRIBUTION

Based on the above discussion, because of the scarcity of the available radio spectrum, mobile networks have been evolved toward improving spectrum utilization to address the ever-increasing high network capacity and data rate demands. Motivating by this fact, in this paper, we present a framework to give a broad overview on how to improve the utilization of the available 28 GHz spectrum allocated to an arbitrary number of MNOs in a country using indoor small cells for 5G and beyond systems. The framework concerns with the improvement of the utilization of the 28 GHz mmWave spectrum countrywide using a number of spectrum allocation techniques, namely SESA, FUSA, and CFSA. A number of well-known spectrum utilization improvement mechanisms such as spectrum trading, spectrum sharing, and spectrum reusing are then exploited into SESA, FUSA, and CFSA techniques in four major-interconnected domains, including time, frequency, power, and space. We derive the system-level average capacity, spectral efficiency (SE), and energy efficiency (EE) performance metrics for SESA, FUSA, and CFSA techniques in each domain using the Equal Likelihood Criterion and the properties of left-justified Pascal's triangle. Extensive system-level numerical and simulation results and analyses are carried out to evaluate the performance of SESA, FUSA, and CFSA in time-domain, frequency-domain, power-domain, and space-domain for an arbitrary country with four MNOs. In addition, we evaluate whether each spectrum allocation technique operating in any domain can achieve the prospective SE and EE requirements for 6G mobile networks.

E. ORGANIZATION

The paper is organized as follows. The system architecture and proposed framework are presented in section II.

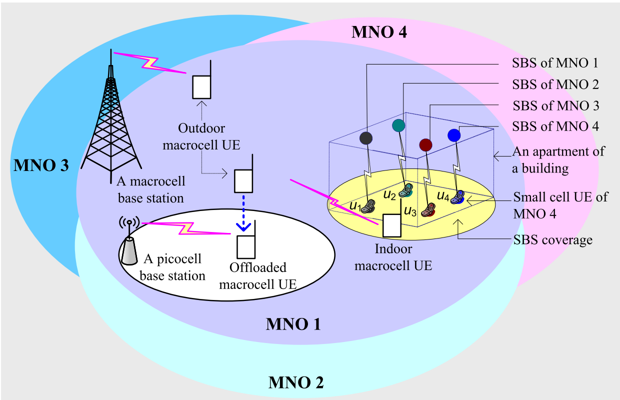

FIGURE 3. A system architecture consisting of four MNOs in a country.

In section III, a mathematical analysis of the proposed framework is carried out for each possible combination of the spectrum allocation techniques in numerous domains. Section IV covers default simulation parameters and assumptions, performance results, and comparisons of SE and EE performances of each spectrum allocation technique in each domain with the prospective SE and EE requirements for 6G mobile networks. We conclude the paper in section V.

F. DECLARATION

The framework presented in this paper gives a general review of our findings, mostly in [4]–[7], [11]–[16], [29]–[36], and [40], [44], [52], relating to improving spectrum utilization of the 28 GHz mmWave systems using indoor small cells in multi-operator network scenarios for 5G and beyond mobile systems. In doing so, we use the Equal Likelihood Criterion and the properties of left-justified Pascal's triangle to derive closed-form solutions with a view to summarizing those findings in a unified manner for each spectrum allocation technique in each domain of the framework in terms of the system-level average capacity, SE, and EE performance metrics. Though relevant mathematical analysis is carried out to justify major statements and issues to keep the paper self-contained, due to its dependency on findings in previous works mentioned above, we may refer to the corresponding previous works to justify several statements and issues without further reproductions or proofs in this paper to avoid redundancy and keep it concise. Finally, due to its inherent quantitative nature, as well as mostly being review type, some materials of the paper, in terms of, e.g., text, equations, figures, tables, notations, and abbreviations, may be found merged with the aforementioned previous works, however, with relevant citations.

II. SYSTEM ARCHITECTURE AND PROPOSED FRAMEWORK

A. SYSTEM ARCHITECTURE

The system architecture consists of an arbitrary number of O MNOs in a country, which is shown in Fig.3 for $O = 4$. Like [14], due to considering a similar architectural feature for each MNO, only one MNO (e.g., MNO 1) is shown in detail in Fig.3. We consider one macrocell base station (MBS) per MNO, and a number of picocell base stations (PBSs) and small cell base stations (SBSs) are deployed within the coverage of the MBS. Each PBS offloads a certain amount of the macrocell traffic only in outdoor environments, whereas each SBS serves traffic only in indoor environments. All SBSs are deployed on different floors one per apartment within a number of multistory buildings located over the macrocell coverage. Though in practice, an SBS can serve multiple users simultaneously, we limit the maximum number of users that an SBS can serve at a time to one to take advantage of the system-level modeling (due to its insignificant variation with the number of users served simultaneously by an SBS) for the purpose of simplicity in finding closed-form solutions, which we detail further in Remark 3. The MBS and PBSs operate at the 2 GHz microwave spectrum, whereas all SBSs operate at the 28 GHz mmWave spectrum.

B. PROPOSED FRAMEWORK

Figure 4 shows a generic framework proposed to improve the mmWave spectrum utilization using indoor small cells in a multi-operator network scenario. Since the major carrier frequencies of 5G in the mmWave band ranges from 25 to 39 GHz (even though the use of even higher frequencies is under consideration for future) [37], the signal propagation characteristics do not change significantly within this range such that the framework can be easily applicable for all existing mmWave bands. Though the framework can be equally applicable to other mmWave bands, we consider the 28 GHz mmWave spectrum band in this paper. The proposed framework explores the available 28 GHz mmWave spectrum specified for a country in two levels. In the primary-level (i.e., Level 1), the full mmWave spectrum in a country is considered allocating to all MNOs of the country. Without the loss of generality, we consider three spectrum allocation techniques for the licensed mmWave countrywide, namely SESA, FUSA, and CFSA.

In SESA, each MNO in a country is allocated to an equal amount of the countrywide licensed spectrum, typically, for the long-term. The amount of spectrum allocated to any MNO does not change (i.e., static) and cannot be shared (i.e., dedicated) with other MNOs in the country, regardless of how the user demand of any MNO changes, over the entire spectrum licensing/renewal term. The major pitfall of SESA is that it is not adaptive to a change in the user demand of an MNO due to its static and dedicated features. However, SESA takes advantage of its simplicity in implementation.

In FUSA, however, each MNO is allocated to an unequal amount of the countrywide licensed spectrum corresponding to its number of subscribers at any spectrum renewal term t_r such that each MNO is allocated to its required amount of the mmWave spectrum to serve its user demand. Hence, FUSA is adaptive (i.e., dynamic) to a change in the user demand of an MNO and an MNO can trade its mmWave spectrum

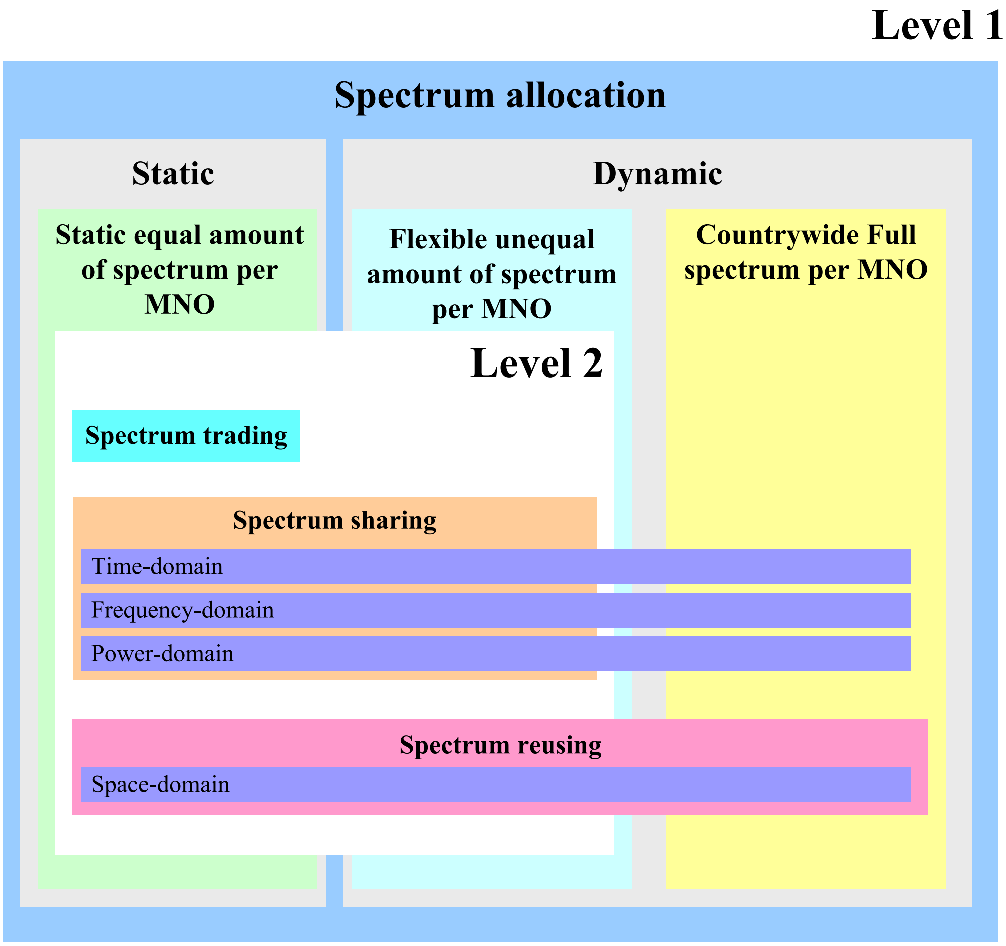

FIGURE 4. A framework to improve mmWave spectrum utilization in multi-operator networks.

with another MNO in the country. However, this approach suffers from computational complexity and an excessive amount of the control signaling overheads on the network. Note that the degree of dynamics of FUSA is a trade-off between the value of t_r and the control signaling overheads generated on the network. Typically, the smaller the value of t_r, the higher the amount of control signaling overheads and vice versa.

Finally, in CFSA, the full spectrum of a country is allocated to each MNO subject to satisfying CCI among user equipments (UEs) of different MNOs. CCI can be generated in either time, frequency, or power domains. CFSA takes advantage of allocating the maximum amount of the countrywide full mmWave spectrum to each MNO when no CCI exists, whereas a minimum amount of spectrum corresponding to its subscribers with respect to that of all MNOs like FUSA when CCI is the maximum. Since, however, the allocated spectrum to each MNO in CFSA is updated more frequently than that in FUSA and SESA, CFSA suffers the most from the complexity in its implementation, as well as the generated control signaling overheads to manage CCI.

Overall, the cost and the complexity in implementation versus the degree of dynamics to update the mmWave spectrum of MNOs and the generated control signaling overheads on the networks play a vital role in considering an appropriate spectrum allocation technique aforementioned. Figure 5 shows an illustration of Level 1 SESA, FUSA, and CFSA techniques.

In secondary-level (i.e., Level 2), the allocated mmWave spectrum in the primary-level to SESA, FUSA, and CFSA is further exploited to increase the spectrum utilization. More specifically, since the spectrum is allocated to an MNO irrespective of its actual user demand in SESA, Level 2 spectrum trading can be employed only to SESA such that each MNO in a country can satisfy its user demand. In secondary-spectrum trading, an MNO can take a lease of a part of the allocated spectrum from another MNO exclusively for a certain agreement term, t_r, at the cost of the leased spectrum fees. Typically, an MNO with unused or underutilized spectrum can sell its licensed spectrum to another MNO with a shortage of spectrum to serve its user demand such that the overall countrywide spectrum utilization can be improved.

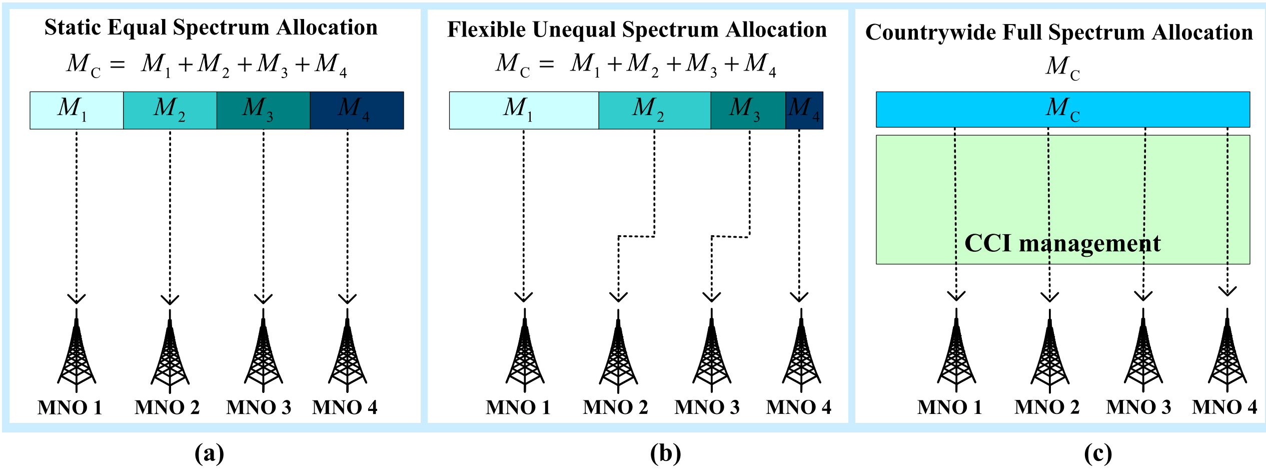

FIGURE 5. An illustration of spectrum allocation techniques in level 1 for a country with four MNOs 1, 2, 3, and 4 at any term t_r. (a) SESA with each MNO allocated to an equal amount of spectrum $M_1 = M_2 = M_3 = M_4 = M = (M_C/4)$. (b) FUSA with the number of subscribers of 40%, 30%, 20%, and 10%, respectively, of the total number of subscribers countrywide for MNO 1, MNO 2, MNO 3, and MNO 4. (c) CFSA with each MNO allocated to the countrywide full mmWave spectrum M_C.

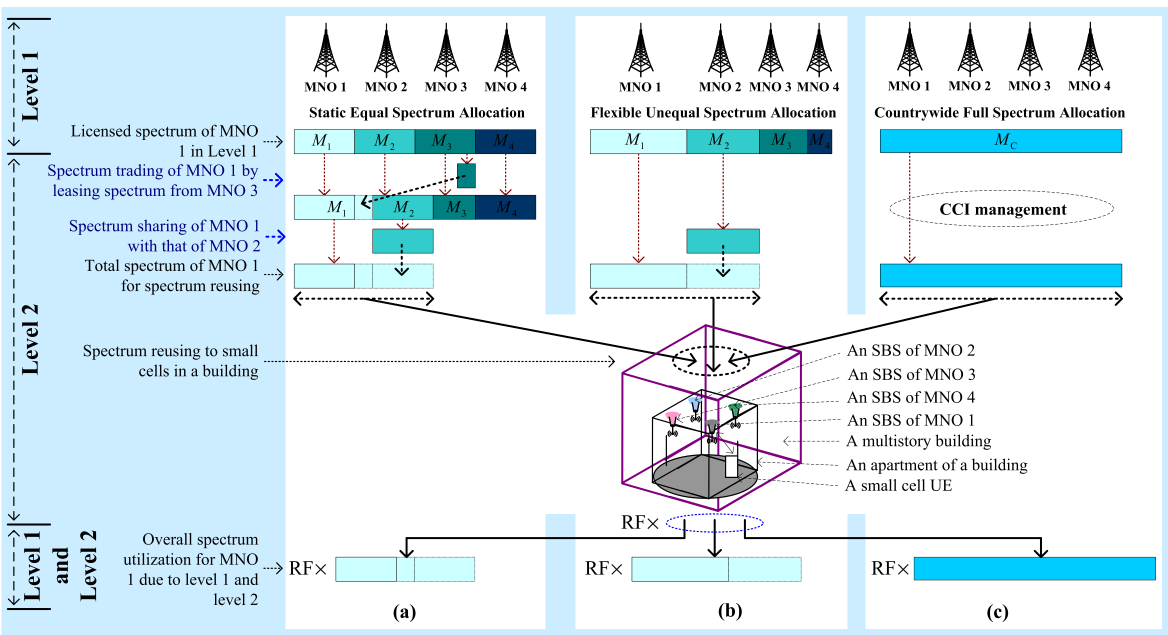

FIGURE 6. An illustration of the application of Level 2 spectrum exploitation to (a) SESA, (b) FUSA, and (c) CFSA in Level 1 at any term t_r.

Further, the allocated spectrum of one MNO can be shared with another MNO in SESA and FUSA such that Level 2 spectrum sharing among MNOs can be employed to both SESA and FUSA by exploiting in either time-domain, frequency-domain, or power-domain to address CCI among MNOs. There are numerous approaches available in the existing literature for sharing the spectrum between MNOs [38] subject to satisfying CCI constraints. Moreover, since the countrywide spectrum in SESA, FUSA, and CFSA can be reused in space subject to satisfying a minimum CCI, Level 2 spectrum reusing technique can be employed to all SESA, FUSA, and CFSA techniques by exploiting the space-domain. For example, by forming a three-dimensional cluster of small cells one per apartment within a building subject to satisfying a minimum CCI between co-channel small cell base stations (BSs), the same spectrum allocated in the primary-level can be reused more than once to small cells per building to increase the utilization of the same spectrum per MNO as shown in Fig.6.

Note that since the countrywide full spectrum is available to each MNO, the spectrum trading in level 2 cannot be applied to CFSA. Figure 6 shows an example use of the Level 2 mmWave spectrum exploitation in SESA, FUSA, and CFSA techniques in level 1 at any term t_r for MNO 1. For spectrum sharing, the spectrum of one MNO is allowed to share with another MNO subject to satisfying CCI in TD, FD, and PD. For spectrum trading, a certain percentage (e.g., 30%) of the allocated spectrum of MNO 3 is considered leasing to MNO 1 for SESA. Table 1 shows a comparison among SESA, FUSA, and CFSA techniques of the proposed framework.

Remark 1: According to [39], since the efficient use of spectrum is influenced mainly by the composite bandwidth-space-time domain, the measure of spectrum utilization, also termed as spectrum utilization factor, should reflect these considerations, i.e. the frequency bandwidth, the time, and the geographic space. Accordingly, in the proposed framework to improve mmWave spectrum utilization (Fig.4), Level 1 spectrum allocation and Level 2 spectrum sharing and spectrum trading address the effect of both frequency and time, whereas Level 2 spectrum reusing address the effect of space such that aggregately Level 1 and Level 2 of the proposed framework takes into account of all the factors (i.e., the frequency bandwidth, the time, and the geographic space) affecting the measure of spectrum utilization.

III. MATHEMATICAL ANALYSIS

Assume that the maximum number of MNOs in a country is O such that $o \in \boldsymbol{O} : \boldsymbol{O} = \{1, 2, \ldots, O\}$. Let N_{C} denote the total number of subscribers countrywide at any licensed renewal term t_{r}. Let M_{C} denote the total amount of mmWave spectrum countrywide defined in terms of the number of resource blocks (RBs) where an RB is equal to 180 kHz. Assume that N_o denotes the number of subscribers at any term t_{r} and M_o denotes the amount of mmWave spectrum allocated to an MNO o in the primary-level such that $\sum_o^O N_o \leq N_{\mathrm{C}}$ and $\sum_o^O M_o \leq M_{\mathrm{C}}$.

A. SPECTRUM TRADING IN SESA

The spectrum trading applies only to SESA due to allocating the same amount of the spectrum to each MNO in SESA even though the actual user demand may vary from one MNO to another. Hence, to overcome the shortage of spectrum of an MNO o allocated in the primary-level, MNO o may take a lease of a certain portion of the spectrum from another MNOs $O\backslash o$ with unused or underutilized spectrum. To define the amount of the spectrum required by MNO o, following [6], we assume that the required amount of the spectrum of MNO o to serve its user demand is proportional to its number of subscribers at any t_{r}. Hence, the required amount of the spectrum of MNO o at any t_{r} is given by [6],

$$M_o^{\mathrm{req}} = (N_o/N_{\mathrm{C}}) \times M_{\mathrm{C}} \tag{1}$$

Recall that M_o denotes the actual amount of the spectrum allocated to MNO o to serve its user demand at the primary-level. Then, the spectrum of MNO o that needs to be traded or leased from other MNOs in the secondary-level spectrum trading at any t_{r} can be expressed as follows [6].

$$M_o^{\mathrm{trd}} = \left(M_o^{\mathrm{req}} - M_o\right) \tag{2}$$

If $M_o^{\mathrm{req}} > M_o$ in (2), M_o^{trd} is positive, which indicates the amount of the surplus spectrum of MNO o even after addressing its user demand at any t_{r}. Likewise, a negative value of M_o^{trd} indicates the amount of the shortage spectrum of MNO o to address its user demand. Note that the amount of the traded spectrum M_o^{trd} for MNO o in (2) is updated iteratively at each term t_{r}. Hence, the system-level aggregate average capacity of an SBS s, as well as all SBSs S_{F} per building, of all MNOs at any t_{r} in SESA with employing the spectrum trading mechanism can be expressed as follows.

$$\sigma_{\mathrm{SESA},O,s}^{\mathrm{ST}} = \sum\nolimits_{o=1}^{O} \sum_{t \in \boldsymbol{T}} \sum\nolimits_{i=1}^{(M_o + M_o^{\mathrm{trd}})} \sigma_{o,s,t,i}\left(\rho_{o,s,t,i}\right) \tag{3}$$

$$\sigma_{\mathrm{SESA},O,S_{\mathrm{F}}}^{\mathrm{ST}} = \sum\nolimits_{s=1}^{S_{\mathrm{F}}} \sigma_{\mathrm{SESA},O,s}^{\mathrm{ST}} \tag{4}$$

Remark 2: Note that we consider that each MNO is allocated to the required amount of spectrum corresponding to its number of subscribers before exploring the dynamic spectrum sharing. To address so, we consider secondary spectrum trading in SESA so that the required spectrum per MNO can satisfy its user demand. However, for FUSA, since the spectrum is allocated to an MNO proportional to its number of subscribers, no spectrum trading is required to address in FUSA. To improve the spectrum utilization further, the dynamic spectrum sharing mechanism using the Equal Likelihood Criterion is applied to both SESA and FUSA.

B. SPECTRUM SHARING IN SESA AND FUSA

Recall that, in SESA, each MNO is allocated to an equal amount of spectrum, denoted as M in RBs, in the primary-level regardless of its actual user demand for a certain renewal term t_{r}(i.e., $\forall o M_o = M$). On the contrary, in FUSA, an MNO o is allocated to the amount of the spectrum compliant with the number of its subscribers N_o for t_{r}(i.e., $\forall o M_o = (N_o/N_{\mathrm{C}}) \times M_{\mathrm{C}}$) [14]. Since the user demand of any MNO is different from that of other MNOs $\boldsymbol{O}\backslash o$, which may change over time and space, the allocated spectrum of an MNO o in the primary-level can be shared in time, frequency, and power domains with the other MNOs $O\backslash o$ in a country, which we describe in what follows.

1) TD AND FD SPECTRUM SHARING

The allocated spectrum to an MNO o in the primary-level can be shared with indoor SBSs of any other MNOs $\boldsymbol{O}\backslash o$ in the secondary-level (Level 2) if the following condition is satisfied [40]. *The spectrum of an MNO o (termed as a primary MNO) can only be shared with the SBSs of any other MNOs $\boldsymbol{O}\backslash o$ (termed as a secondary MNO) in a building as long as no UE of the primary MNO does exist within the building to avoid CCI generated between the UEs of the primary and secondary MNOs.*

Now, following [41]–[43], we consider that an SBS can serve one UE at a time. Moreover, we consider that each combination of the coexistence of small cell UEs of other MNOs $\boldsymbol{O}\backslash o$ (one UE from each MNO) with a UE of an MNO o in an apartment is equally likely over any observation time

TABLE 1. **A comparison among SESA, FUSA, and CFSA techniques of the proposed framework.**

Attribute	SESA	FUSA	CFSA
Spectrum allocation	Static	Dynamic	Dynamic
Allocated spectrum per MNO	Equal	Unequal (depends on the user statistics)	Countrywide full
Coordination for the spectrum allocation	Not needed	Distributed and per term t_r basis	Centralized and per TTI t basis
Spectrum trading	Yes	No	No
Spectrum sharing	Yes	Yes	Yes
Spectrum reusing	Yes	Yes	Yes
Spectrum renewal term (t_r)	Long (e.g., 5 to 10 years)	Short (e.g., 6 to 12 months)	Short (e.g., 6 to 12 months)

$|\boldsymbol{T}| = Q$ such that any combination of the coexistence of UEs occurs with a probability of $\frac{Q}{2^{O-1}}$. Then, each of the above possible combinations for the coexistence of the UE u_1 of MNO $o = 1$ with other UEs $\boldsymbol{O}\backslash o$ (i.e., u_2, u_3, and u_4) in an apartment corresponds to the shared spectrum (as given in column 5) and the total spectrum (as given in column 6) of Table 2 for the UE u_1.

Hence, using Table 2, in SESA, for a UE of any MNO o allocated to an equal amount of spectrum of M, the components of the shared spectra can be expressed as $\{0, M, 2M, \ldots, (n-1)M, nM\}$ where $n = (O-1)$. Note that the same component of the shared spectrum exists more than once in Table 2 such that each multiplier corresponding to the respective component of the shared spectrum can be defined by a Binomial coefficient $\binom{n}{k}$ of row n of the left-justified Pascal's triangle given in Table 3, where $n \geq k \geq 0$ [40]. Hence, the complete set of components of the shared spectrum, where each component of the shared spectrum is scaled by its corresponding multiplier, for a UE of an MNO o (shown in Table 2) can be expressed as follows [40]

$$\left\{\left(\binom{n}{0} \times 0\right), \left(\binom{n}{1} \times (M)\right), \left(\binom{n}{2} \times (2M)\right), \ldots, \left(\binom{n}{n} \times (nM)\right)\right\}$$

shown in Table 3.

The aggregate capacity of an SBS s, as well as all SBSs S_{F} for a building,of MNO o at any t_r for SESA, can be given by [40],

$$\sigma_{\mathrm{SESA},s,o}^{\mathrm{SS,TD}} = \sum_{t \in \boldsymbol{T}} \sum\nolimits_{i=1}^{M} \sigma_{t,i,o}\left(\rho_{t,i,o}\right) + \sum_{k=1}^{O-1} \binom{O-1}{k} \times \left(\sum\nolimits_{t=1}^{(Q/2^{O-1})} \sum\nolimits_{i=1}^{kM} \sigma_{k,t,i,o}\left(\rho_{k,t,i,o}\right)\right) \tag{5}$$

$$\sigma_{\mathrm{SESA},o,S_{\mathrm{F}}}^{\mathrm{SS,TD}} = \sum\nolimits_{s=1}^{S_{\mathrm{F}}} \sigma_{\mathrm{SESA},o,s}^{\mathrm{SS,TD}} \tag{6}$$

TABLE 2. **The equally likely coexistence and the corresponding shared spectrum for u_1 of MNO 1 in SESA for $O = 4$ [12].**

Coexistence for u_1				Spectrum for u_1	
u_1	u_2	u_3	u_4	Shared	Total
0	0	0	0	Not applicable due to nonexistence of u_1	
0	0	0	1		
0	0	1	0		
0	0	1	1		
0	1	0	0		
0	1	0	1		
0	1	1	0		
0	1	1	1		
1	0	0	0	$3M$	$4M$
1	0	0	1	$2M$	$3M$
1	0	1	0	$2M$	$3M$
1	0	1	1	M	$2M$
1	1	0	0	$2M$	$3M$
1	1	0	1	M	$2M$
1	1	1	0	M	$2M$
1	1	1	1	0	M

Hence, the countrywide aggregate capacity of all MNOs O for a building of SBSs for SESA is given by,

$$\sigma_{\mathrm{SESA},O,S_{\mathrm{F}}}^{\mathrm{SS,TD}} = \sum\nolimits_{o=1}^{O} \sum\nolimits_{s=1}^{S_{\mathrm{F}}} \sigma_{\mathrm{SESA},o,s}^{\mathrm{SS,TD}} \tag{7}$$

For FUSA, since an MNO o is allocated to an amount of spectrum different from that of the others $\boldsymbol{O}\backslash o$, the total amount of the shared spectrum for any UE of an MNO o can be found by estimating the shared spectrum component corresponding to each possible combination of all UEs in an apartment. In this regard, Pascal's triangle can be used to find the components of the shared spectrum. This is because the countrywide performance of all MNOs O does not vary with whether each MNO is allocated to the same or a different amount of the spectrum from that of the others. Hence, following Pascal's triangle, in an indirect way, we can find the sum of the total amount of the shared spectrum for a UE of each MNO o such that the countrywide average capacity for all MNOs O for a building of SBSs in FUSA is given by (7) as well [40], i.e.,

$$\sigma_{\mathrm{FUSA},O,S_{\mathrm{F}}}^{\mathrm{SS,TD}} = \sigma_{\mathrm{SESA},O,S_{\mathrm{F}}}^{\mathrm{SS,TD}} \tag{8}$$

Like FUSA, when considering the spectrum trading in SESA, the total spectrum of each MNO is no longer remains the same (i.e., M). Instead, due to the secondary-level spectrum trading, the spectrum allocated to each MNO in the primary-level in SESA is reassigned among MNOs such that the total spectrum of one MNO differs from another as we have described before while discussing the spectrum trading among MNOs. However, like FUSA, using Pascal's triangle as described above, the countrywide average capacity of all MNOs O for a building of SBSs in SESA when employing the spectrum trading mechanism expressed in (4) can also be given by (8).

2) PD SPECTRUM SHARING

CCI can also be managed by controlling the transmission power of small cells of each MNO. In this regard, cognitive radio is an effective technology to control CCI in the power-domain. More specifically, by employing techniques such as the interweave spectrum access and the underlay spectrum access, CCI among small cells of different MNOs can be managed. Moreover, by employing both the interweave spectrum and the underlay spectrum access (also termed as the hybrid interweave-underlay spectrum access), we can also manage CCI.

Since in SESA and FUSA, the spectrum is allocated in the primary-level orthogonally to all MNOs in a country, the same CCI management principle can be applied to SESA and FUSA. In such a case, following [34], to share the spectrum of one MNO with indoor SBSs of another MNO, CCI can be managed in the power-domain by controlling the transmission power of an SBS as follows. *The spectrum allocated to an MNO o in the primary-level can be allowed to share with a small cell of any MNOs* $\boldsymbol{O}\backslash o$ *by operating its small cells at the maximum transmission power if no small cell UE of MNO o is present, whereas at a reduced transmission power if a small cell UE of MNO o is present, within the coverage of the corresponding small cell of MNOs* $\boldsymbol{O}\backslash o$ *in a building to avoid CCI. The reduced transmission power is subjected to satisfying the predefined maximum allowable interference level of MNO o.*

Note that the above CCI management explores both the interweave and underlay spectrum access techniques in a sense that the interweave spectrum access is explored by operating small cells of secondary MNOs $\boldsymbol{O}\backslash o$ at the maximum transmission power and the underlay spectrum access is explored by operating the same small cells at a reduced transmission power. These help small cells of the secondary MNOs $\boldsymbol{O}\backslash o$ opportunistically serve high capacity at the maximum transmit power during the absence of a UE of the primary MNO o, as well as continue an uninterrupted service at reduced power during the presence of a UE of MNO o while sharing their spectra with MNO o, resulting in improving the spectrum utilization further.

Assume that P_{m} and P_{r} denote, respectively, the maximum transmission power and the reduced transmission power of an SBS of MNO o when employing the interweave and underlay spectrum access techniques, respectively. Let $\rho^{\mathrm{iw}}_{o,t,i}$ and $\sigma^{\mathrm{iw}}_{o,t,i}$ denote, respectively, the SINR and the corresponding link capacity in any TTI $= t$ at RB $= i$ when an SBS is operating at P_{m}. Likewise, let $\rho^{\mathrm{ul}}_{o,t,i}$ and $\sigma^{\mathrm{ul}}_{o,t,i}$ denote, respectively, the SINR and the corresponding link capacity it any TTI $= t$ at RB$= i$ when an SBS is operating at P_{r}.

TABLE 3. Left-justified Pascal's triangle to find a set of multipliers to the respective shared spectrum components [40].

O	n=O-1	Multiplication entry for the components of the shared spectra						2^n
		0	M	$2M$	$3M$	$4M$	$5M$	
1	0	1						1
2	1	1	1					2
3	2	1	2	1				4
4	3	1	3	3	1			8
5	4	1	4	6	4	1		16
6	5	1	5	10	10	5	1	32

Now, using Table 2, we can develop Table 4 [34] as follows such that following Table 4, the aggregate capacity of MNO o at any t_{r} for SESA when employing only the interweave spectrum access technique is given for an SBS s, as well as all SBSs S_{F} per building, as follows [40].

$$\sigma^{\mathrm{SS,PD,iw}}_{\mathrm{SESA},o,s} = \sum\nolimits_{t=1}^{(Q/2^{O-1})} \sum\nolimits_{i=1}^{M} \sigma^{\mathrm{iw}}_{o,t,i}\left(\rho^{\mathrm{iw}}_{o,t,i}\right) + \sum_{k=1}^{O-1} \binom{O-1}{k} \times \left(\sum\nolimits_{t=1}^{(Q/2^{O-1})} \sum\nolimits_{i=1}^{kM} \sigma^{\mathrm{iw}}_{o,k,t,i}\left(\rho^{\mathrm{iw}}_{o,k,t,i}\right)\right) \tag{9}$$

$$\sigma^{\mathrm{SS,PD,iw}}_{\mathrm{SESA},o,S_{\mathrm{F}}} = \sum\nolimits_{s=1}^{S_{\mathrm{F}}} \sigma^{\mathrm{SS,PD,iw}}_{\mathrm{SESA},o,s} \tag{10}$$

Similarly, when employing only the underlay spectrum access technique, the aggregate capacity of MNO o at any t_{r} for SESA is given for an SBS s, as well as all SBSs S_{F} per building, as follows [40],

$$\sigma^{\mathrm{SS,PD,ul}}_{\mathrm{SESA},o,s} = \sum\nolimits_{t=1}^{(Q/2^{O-1})} \sum\nolimits_{i=1}^{M} \sigma^{\mathrm{iw}}_{o,t,i}\left(\rho^{\mathrm{iw}}_{o,t,i}\right) + \sum_{k=1}^{O-1} \binom{O-1}{k} \times \left(\sum\nolimits_{t=1}^{(Q/2^{O-1})} \sum\nolimits_{i=1}^{kM} \sigma^{\mathrm{ul}}_{o,k,t,i}\left(\rho^{\mathrm{ul}}_{o,k,t,i}\right)\right) \tag{11}$$

$$\sigma^{\mathrm{SS,PD,ul}}_{\mathrm{SESA},o,S_{\mathrm{F}}} = \sum\nolimits_{s=1}^{S_{\mathrm{F}}} \sigma^{\mathrm{SS,PD,ul}}_{\mathrm{SESA},o,s} \tag{12}$$

However, following Table 4 [34], when employing both the interweave, as well as the underlay, spectrum access techniques, the aggregate capacity of MNO o at any t_{r} for SESA can be given for an SBS s, as well as all SBSs S_{F} per building, as follows.

$$\sigma^{\mathrm{SS,PD,hy}}_{\mathrm{SESA},o,s} = \sum\nolimits_{t=1}^{Q} \sum\nolimits_{i=1}^{M} \sigma^{\mathrm{iw}}_{o,t,i}\left(\rho^{\mathrm{iw}}_{o,t,i}\right)$$

TABLE 4. Coexistence and shared spectrum for UE u_1 of MNO 1 for the interweave and underlay spectrum access techniques in a country of four MNOS 1, 2, 3, and 4 [34].

u_1	u_2	u_3	u_4	Shared spectrum for u_1		Licensed spectrum for u_1
				Interweave	Underlay	Both interweave and underlay
0	0	0	0	Not applicable due to the nonexistence of u_1		
0	0	0	1			
0	0	1	0			
0	0	1	1			
0	1	0	0			
0	1	0	1			
0	1	1	0			
0	1	1	1			
1	0	0	0	$3M$	0	M
1	0	0	1	$2M$	M	M
1	0	1	0	$2M$	M	M
1	0	1	1	M	$2M$	M
1	1	0	0	$2M$	M	M
1	1	0	1	M	$2M$	M
1	1	1	0	M	$2M$	M
1	1	1	1	0	$3M$	M

$$+\sum_{k=1}^{O-1}\binom{O-1}{k} \times\left(\sum_{t=1}^{(Q/2^{O-1})}\sum_{i=1}^{kM}\left(\begin{array}{l}\sigma^{\text{iw}}_{o,k,t,i}\left(\rho^{\text{iw}}_{o,k,t,i}\right)\\ +\sigma^{\text{ul}}_{o,k,t,i}\left(\rho^{\text{ul}}_{o,k,t,i}\right)\end{array}\right)\right) \tag{13}$$

$$\sigma^{\text{SS,PD,hy}}_{\text{SESA},o,S_{\text{F}}}=\sum_{s=1}^{S_{\text{F}}}\sigma^{\text{SS,PD,hy}}_{\text{SESA},o,s} \tag{14}$$

Hence, the countrywide aggregate capacity of all MNOs O for a building of SBSs is given by,

$$\sigma^{\text{SS,PD,hy}}_{\text{SESA},O,S_{\text{F}}}=\sum_{o=1}^{O}\sum_{s=1}^{S_{\text{F}}}\sigma^{\text{SS,PD,hy}}_{\text{SESA},o,s} \tag{15}$$

Now, following the same explanation for (8), when employing both the interweave, as well as the underlay, spectrum access techniques, the countrywide average capacity for all MNOs O for a building of SBSs at any t_{r} for FUSA is given by,

$$\sigma^{\text{SS,PD,hy}}_{\text{FUSA},O,S_{\text{F}}}=\sigma^{\text{SS,PD,hy}}_{\text{SESA},O,S_{\text{F}}} \tag{16}$$

C. SPECTRUM SHARING IN CFSA

Recall that, in CFSA, an MNO o in a country is allocated to the countrywide full spectrum dynamically to operate its small cells located within each building subject to managing CCI with small cells of other MNOs $\boldsymbol{O}\backslash o$ for t_{r}. Small cells or their UEs of an MNO o can help detect the existence of small cell UEs of other MNOs $\boldsymbol{O}\backslash o$ to manage CCI due to operating at the same countrywide spectrum by all MNOs. In CFSA, CCI can be managed in time, frequency, and power domains, which are described in the following.

1) TD AND FD SPECTRUM SHARING

In TD, FD, and PD for CFSA, following SESA and FUSA [44], we also consider that each combination of the coexistence of small cell UEs of interferer MNOs $\boldsymbol{O}\backslash o$ with a small cell UE of an MNO o in an apartment is equally likely during any observation time $|\boldsymbol{T}| = Q$ such that each combination of the coexistence of small cell UEs of interferer MNOs $\boldsymbol{O}\backslash o$ occurs with a probability of $\frac{Q}{2^{O-1}}$.

Let k be a set of positive integers (representing the number of small cell UEs of interferer MNOs $\boldsymbol{O}\backslash o$ in an apartment) such that $0 \leq k \leq (|\boldsymbol{O}|-1)$. Then, following the left-justified Pascal's triangle [45], the duration (in TTIs) of a small cell s of MNO o corresponding to k can be given in TD by,

$$t_{o,k}=\binom{O-1}{k}\times\left(\frac{Q}{2^{O-1}}\right) \tag{17}$$

However, in FD CFSA, we assume that the countrywide full-spectrum is allocated to an SBS of MNO o in an apartment in proportionate to the number of interferer small cell UEs of other MNOs $\boldsymbol{O}\backslash o$ exists in any TTI $t_{o,k}$. Hence, using (17) and for $0 \leq k \leq (|\boldsymbol{O}|-1)$, the amount of spectrum allocated to an SBS of an MNO o in an apartment in RBs corresponding to $t_{o,k}$ at any t_{r} can be given in FD by,

$$M_{o,k}=\frac{M_{\text{C}}}{(k+1)}: 0\leq k\leq (|\boldsymbol{O}|-1) \tag{18}$$

Now, due to employing $t_{o,k}$ in (17) for the TD and $M_{o,k}$ in (18) for the FD, the aggregate capacity of an SBS s, as well as all SBSs S_{F} per building, of MNO o in CFSA at any t_{r} in both TD and FD CCI avoidance are the same, which can be given by,

$$\sigma^{\text{SA,TD}}_{\text{CFSA},o,s}=\sigma^{\text{SA,FD}}_{\text{CFSA},o,s} =\sum_{k=0}^{O-1}\left(\sum_{t=1}^{\left(\binom{O-1}{k}\times\left(\frac{Q}{2^{O-1}}\right)\right)} \times\sum_{i=1}^{M_{o,k}}\sigma_{o,k,t,i}\left(\rho_{o,k,t,i}\right)\right) \tag{19}$$

$$\sigma^{\text{SA,TD}}_{\text{CFSA},o,S_{\text{F}}}=\sigma^{\text{SA,FD}}_{\text{CFSA},o,S_{\text{F}}} =\sum_{s=1}^{S_{\text{F}}}\sum_{k=0}^{O-1}\left(\sum_{t=1}^{\left(\binom{O-1}{k}\times\left(\frac{Q}{2^{O-1}}\right)\right)} \times\sum_{i=1}^{M_{o,k}}\sigma_{o,s,k,t,i}\left(\rho_{o,s,k,t,i}\right)\right) \tag{20}$$

2) PD SPECTRUM SHARING

Like in PD CCI management for SESA and FUSA, assume that in the interweave spectrum access, a small cell of an MNO o operates at the maximum transmission power as long as no small cell UE of other MNOs $\boldsymbol{O}\backslash o$ exists within its coverage. However, with the existence of a small cell UE of any MNOs $\boldsymbol{O}\backslash o$, the small cell of MNO o stops serving its UE. Unlike the interweave spectrum access, using the underlay spectrum access, a small cell of an MNO o can continue serving its UEs simultaneously at a reduced transmission power, subject to satisfying a predefined interference threshold, even at the presence of small cell UEs of MNOs $\boldsymbol{O}\backslash o$.

Recall that P_{m} and P_{r} denote, respectively, the maximum transmission power and the reduced transmission power of a small cell of MNO o. Then, the transmission power of any small cell of MNO o can be expressed for the interweave spectrum access and the underlay spectrum access as follows.

$$P_o = \left\{ \begin{array}{ll} P_{\mathrm{m}}, & \text{for interweave spectrum access} \\ P_{\mathrm{r}}, & \text{for underlay spectrum access} \end{array} \right\} \quad (21)$$

Let $\boldsymbol{U}$ denote a set of interferer small cell UEs of MNOs $O\backslash o$ (one UE from each MNO) such that $u_o \in \boldsymbol{U_o} = \{\boldsymbol{O}\backslash o\}$. Unlike SESA and FUSA, all MNOs operate at the countrywide full spectrum in CFSA. Hence, if a small cell of an MNO o is operating under the underlay access, with an increase in the number of interferers, i.e., small cell UEs of MNOs $O\backslash o$, the aggregate interference from one small cell to another increase. This causes, unlike SESA and FUSA, the transmission power P_{r} of each small cell of all MNOs in CFSA to be adjusted as follows such that the aggregate interference power does not exceed the interference threshold (i.e., the maximum value of CCI power) I_{m} [44].

$$P_{\mathrm{r}} = \left\{ \begin{array}{cc} (\alpha_1 \times P_{\mathrm{m}}), & \text{for } |\boldsymbol{U_o}| = 1 \\ \vdots & \vdots \\ \left(\alpha_{(|\boldsymbol{O}|-1)} \times P_{\mathrm{m}}\right), & \text{for } |\boldsymbol{U_o}| = (|\boldsymbol{O}|-1) \end{array} \right\} \quad (22)$$

where $\alpha_1, \alpha_2, \ldots \alpha_{(|\boldsymbol{O}|-1)}$ are scalar quantities and $\alpha_1 > \alpha_2 > \cdots > \alpha_{(|\boldsymbol{O}|-1)}$ such that $\sum_{x=1}^{(|\boldsymbol{O}|-1)} (\alpha_x \times P_{\mathrm{m}}) \leq I_{\mathrm{m}}$ as each small cell of all MNOs causes CCI mutually to one another when employing the underlay spectrum access technique.

Now using (21) and (22), the transmission power of a small cell of MNO o can be written as follows.

$$P_o = \left\{ \begin{array}{cc} P_{\mathrm{m}}, & \text{for } |\boldsymbol{U_o}| = 0 \\ (\alpha_1 \times P_{\mathrm{m}}), & \text{for } |\boldsymbol{U_o}| = 1 \\ \vdots & \vdots \\ \left(\alpha_{(|\boldsymbol{O}|-1)} \times P_{\mathrm{m}}\right), & \text{for } |\boldsymbol{U_o}| = (|\boldsymbol{O}|-1) \end{array} \right\} \quad (23)$$

Hence, using (17) for an equally likely criterion for the coexistence of small cell UEs of interferer MNOs $\mathbf{O}\backslash$o with a small cell UE of an MNO o in an apartment in PD, the aggregate capacity of an SBS s, as well as all SBSs S_{F} per building, of MNO o at any t_{r} in CFSA can be given by,

$$\sigma^{\mathrm{SA,PD}}_{\mathrm{CFSA},o,s} = \sum_{k=0}^{O-1} \left(\sum\nolimits_{t=1}^{\left(\binom{O-1}{k}\times\left(\frac{Q}{2^{O-1}}\right)\right)} \times \sum\nolimits_{i=1}^{M_{\mathrm{C}}} \sigma_{o,k,t,i}\left(\rho_{o,k,t,i}\right) \right) \quad (24)$$

$$\sigma^{\mathrm{SA,PD}}_{\mathrm{CFSA},o,S_{\mathrm{F}}} = \sum\nolimits_{s=1}^{S_{\mathrm{F}}} \sigma^{\mathrm{SA,PD}}_{\mathrm{CFSA},o,s} \quad (25)$$

D. SPECTRUM REUSING IN SESA, FUSA, AND CFSA

The countrywide full spectrum in CFSA and a fraction of the countrywide spectrum either equal in SESA or unequal in FUSA, allocated to an MNO o in the primary-level using either TD, FD, or PD CCI management can be exploited further in the 3-dimensional (3D) space of a multistory building of small cells. More specifically, by enforcing a maximum CCI, a minimum distance between co-channel small cells (each located in an apartment) can be defined in both the intra-floor and inter-floor levels to form a 3D cluster of small cells within a building. The allocated spectrum per MNO can then be reused to each 3D cluster of small cells to improve the spectrum utilization. Further, since the external wall penetration loss of a building is high enough for a high-frequency mmWave signal, the same spectrum can be reused to small cells in adjacent buildings, resulting in improving the spectrum utilization further. Adopting [46], a minimum distance between co-channel small cells for the 28 GHz mmWave spectrum in the intra-floor level and inter-floor level, respectively, for MNO o at any term t_{r} can be expressed as follows.

$$\Delta_{\mathrm{a}} = \Delta_{\mathrm{m}} \times \left(\Xi_{\mathrm{a}} \Big/ I_{\mathrm{a}}^{\mathrm{thr}}\right)^{(1/1.797)} \quad (26)$$

$$\Delta_{\mathrm{e}} \geq \Delta_{\mathrm{m}} \times \left(\left(\Xi_{\mathrm{e}} \Big/ I_{\mathrm{e}}^{\mathrm{thr}}\right) \Big/ 10^{(\alpha_{\mathrm{f}}(\Delta_{\mathrm{e}})/10)}\right)^{(1/1.797)} \quad (27)$$

where $I_{\mathrm{a}}^{\mathrm{thr}}$ and $I_{\mathrm{e}}^{\mathrm{thr}}$ denote, respectively, intra-floor and inter-floor CCI constraints at a small cell UE. Ξ_{a} and Ξ_{e} denote, respectively, the maximum number of co-channel small cells in the intra-floor level and inter-floor level. Δ_{m} denotes the minimum distance between a co-channel small cell and a small cell UE and $\alpha_{\mathrm{f}}(\Delta_{\mathrm{e}})$ denotes the floor penetration loss at the 28 GHz mmWave spectrum.

Let s_l^{a} and s_l^{e} denote, respectively, the number of small cells corresponding to $\Delta_{\mathrm{a},l}$ and $\Delta_{\mathrm{e},l}$ in a building l such that a 3D cluster consists of $S_{3\mathrm{D},l} = \left(s_l^{\mathrm{a}} \times s_l^{\mathrm{e}}\right)$ small cells. Hence, the same spectrum of MNO o can be reused for each cluster of $\left(s_l^{\mathrm{a}} \times s_l^{\mathrm{e}}\right)$ small cells in a building. Let $S_{\mathrm{F},l}$ denote the maximum number of small cells of MNO o in a building l such that the number of times the same spectrum of MNO o can be reused in building l (i.e., the spectrum reuse factor (RF) for MNO o in building l) can be expressed as follows.

$$\omega_l = \frac{S_{\mathrm{F},l}}{\left(s_l^{\mathrm{a}} \times s_l^{\mathrm{e}}\right)} \quad (28)$$

$$\omega_l = \frac{S_{\mathrm{F},l}}{S_{\mathrm{3D},l}} \tag{29}$$

Let L denote the number of buildings of small cells in a macrocell of MNO o. Then, the spectrum RF for a macrocell of MNO o is given by,

$$\omega_{\mathrm{MC}} = \sum_{l=1}^{L} \omega_l \tag{30}$$

Note that if each building has similar architecture and indoor signal propagation characteristics, then for the same number of small cells per building (i.e., $\forall l S_{\mathrm{F},l} = S_{\mathrm{F}}$) such that $\forall l \omega_l = \omega$ for each MNO o, the spectrum RF for a macrocell of each MNO o is given by,

$$\omega_{\mathrm{MC}} = (L \times \omega) \tag{31}$$

E. SYSTEM-LEVEL AVERAGE CAPACITY, SE AND EE IN SESA, FUSA, AND CFSA

Let M_o^{MC} and N_o^{MC} denote, respectively, the spectrum bandwidth in RBs and the number of UEs of a macrocell of MNO o. Let γ denote SE, and ε denote EE, corresponding to the average capacity σ. Also, let ξ and ς denote, respectively, the SE and EE improvement factors corresponding to the improvement factor for average capacity ζ. Then, the aggregate average capacity of all macrocell UEs can be expressed as follows [32].

$$\sigma_o^{\mathrm{MC}} = \sum_{t \in \boldsymbol{T}} \sum\nolimits_{i=1}^{M_o^{\mathrm{MC}}} \sigma_{o,t,i}\left(\rho_{o,t,i}\right) \tag{32}$$

where σ and ρ are responses over M_o^{MC} RBs in $t \in \boldsymbol{T}$.

1) SYSTEM-LEVEL AVERAGE CAPACITY

Using the proposed framework in Fig.4, the countrywide system-level aggregate average capacity of all MNOs O at any term t_{r} for SESA, FUSA, and CFSA can be expressed in TD as follows.

$$\sigma_{\mathrm{SESA},O}^{\mathrm{TD}} = \sum\nolimits_{o=1}^{O}\left(\sigma_o^{\mathrm{MC}} + \sum\nolimits_{l=1}^{L}\left(\omega_l \times \sum\nolimits_{s=1}^{S_{\mathrm{3D},l}} \sigma_{\mathrm{SESA},o,s}^{\mathrm{SS,TD}}\right)\right) \tag{33}$$

$$\sigma_{\mathrm{FUSA},O}^{\mathrm{TD}} = \sum\nolimits_{o=1}^{O}\left(\sigma_o^{\mathrm{MC}} + \sum\nolimits_{l=1}^{L}\left(\omega_l \times \sum\nolimits_{s=1}^{S_{\mathrm{3D},l}} \sigma_{\mathrm{FUSA},o,s}^{\mathrm{SS,TD}}\right)\right) \tag{34}$$

$$\sigma_{\mathrm{CFSA},O}^{\mathrm{TD}} = \sum\nolimits_{o=1}^{O}\left(\sigma_o^{\mathrm{MC}} + \sum\nolimits_{l=1}^{L}\left(\omega_l \times \sum\nolimits_{s=1}^{S_{\mathrm{3D},l}} \sigma_{\mathrm{CFSA},o,s}^{\mathrm{SA,TD}}\right)\right) \tag{35}$$

Following (33)-(35), the countrywide aggregate capacity of all MNOs O at any term t_{r} for SESA, FUSA, and CFSA can also be expressed in FD and PD.

2) SYSTEM-LEVEL SPECTRAL EFFICIENCY

Since in SESA, FUSA, and CFSA, the countrywide full mmWave spectrum M_{C} is used to serve small cell users of all MNOs at any term t_{r}, the system-level average spectral efficiency in bps/Hz can be found by simply dividing the respective average capacity of each technique in any domain by the sum of the macrocell spectra of all MNOs and the countrywide full mmWave spectrum. For example, the TD average SE in SESA, FUSA, and CFSA techniques can be found, respectively, as follows.

$$\gamma_{\mathrm{SESA},O}^{\mathrm{TD}} = \sigma_{\mathrm{SESA},O}^{\mathrm{TD}} \Big/ \left(\left(M_{\mathrm{C}} + \sum\nolimits_{o=1}^{O} M_o^{\mathrm{MC}}\right) \times Q\right) \tag{36}$$

$$\gamma_{\mathrm{FUSA},O}^{\mathrm{TD}} = \sigma_{\mathrm{FUSA},O}^{\mathrm{TD}} \Big/ \left(\left(M_{\mathrm{C}} + \sum\nolimits_{o=1}^{O} M_o^{\mathrm{MC}}\right) \times Q\right) \tag{37}$$

$$\gamma_{\mathrm{CFSA},O}^{\mathrm{TD}} = \sigma_{\mathrm{CFSA},O}^{\mathrm{TD}} \Big/ \left(\left(M_{\mathrm{C}} + \sum\nolimits_{o=1}^{O} M_o^{\mathrm{MC}}\right) \times Q\right) \tag{38}$$

Like the average capacity, following (36)-(38), the system level average SE of all MNOs O at any term t_{r} for SESA, FUSA, and CFSA can also be expressed in FD and PD.

3) SYSTEM-LEVEL ENERGY EFFICIENCY

a: SESA AND FUSA

For SESA and FUSA, in TD and FD, the components of the shared spectra for a UE of MNO o changes with the change in the presence of UEs of other MNOs $\boldsymbol{O}\backslash$o. However, there is no change in the transmission power of any SBS. Hence, the EE in TD and FD in SESA can be expressed as follows.

$$\varepsilon_{\mathrm{SESA},O}^{\mathrm{TD}} = \frac{\sum\nolimits_{o=1}^{O}\left(\begin{array}{l}\sum\nolimits_{l=1}^{L}\left(\omega_l \times \sum\nolimits_{s=1}^{S_{\mathrm{3D},l}} P_{\mathrm{SC},o,l,s}\right)\\ +\left(S_{\mathrm{P},o} \times P_{\mathrm{PC}}\right) + \left(S_{\mathrm{M},o} \times P_{\mathrm{MC}}\right)\end{array}\right)}{\left(\sigma_{\mathrm{SESA},O}^{\mathrm{TD}} \big/ Q\right)} \tag{39}$$

$$\varepsilon_{\mathrm{SESA},O}^{\mathrm{FD}} = \frac{\sum\nolimits_{o=1}^{O}\left(\begin{array}{l}\sum\nolimits_{l=1}^{L}\left(\omega_l \times \sum\nolimits_{s=1}^{S_{\mathrm{3D},l}} P_{\mathrm{SC},o,l,s}\right)\\ +\left(S_{\mathrm{P},o} \times P_{\mathrm{PC}}\right) + \left(S_{\mathrm{M},o} \times P_{\mathrm{MC}}\right)\end{array}\right)}{\left(\sigma_{\mathrm{SESA},O}^{\mathrm{FD}} \big/ Q\right)} \tag{40}$$

Likewise, following (39) and (40), respectively, the EE in TD and FD in FUSA can be expressed.

Since in PD, the transmission power of an SBS of MNO o changes in accordance with the change in the presence of UEs of other MNOs $\boldsymbol{O}\backslash o$, i.e., an SBS of MNO o operates at the maximum transmission power if no UE of other MNOs $\boldsymbol{O}\backslash o$ is present and at a reduced transmission power when a UE of the shared spectrum of any other MNOs is present. So, for the hybrid interweave-underlay spectrum access, the EE in PD for SESA and FUSA can be expressed as follows. Note that we consider a separate transceiver in SESA and FUSA for the spectrum of each MNO o of each SBS to switch on and off easily to save the transmission power. Hence, there are O transceivers per SBS of MNO o where a transceiver is operating at the licensed spectrum of MNO o itself and the remaining $(O-1)$ transceivers are operating at the shared spectrum of other MNOs $\boldsymbol{O}\backslash o$ such that the average EE in Joules/bit in PD (for the hybrid interweave-underlay spectrum access) in SESA (and FUSA) can be given by, where $P_{\mathrm{SC,m},o,l,s}$, $P_{\mathrm{SC,iw},o,l,s}$, and $P_{\mathrm{SC,ul},o,l,s}$ denote, respectively, the transmission power of an SBS s of MNO o in a building l when operating at the maximum transmission power, the transmission power with employing the interweave spectrum access, and the transmission power with employing the underlay spectrum access such that $P_{\mathrm{SC,iw},o,l,s} = P_{\mathrm{SC,m},o,l,s}$ and $P_{\mathrm{SC,ul},o,l,s} < P_{\mathrm{SC,m},o,l,s}$. Similarly, following (41), as shown at the bottom of the page, the average EE in PD when employing either the interweave spectrum access or the underlay spectrum access for SESA and FUSA can be expressed.

b: CFSA

Following (33)-(35), the countrywide aggregate capacity of all MNOs O at any term t_r for CFSA can be expressed in TD, FD, and PD. Now, EE in TD (and FD) in CFSA can be expressed as follows. (42), as shown at the bottom of the next page, where $\sigma^{\mathrm{TD}}_{\mathrm{CFSA},O}$ denotes the countrywide aggregate capacity of all MNOs O at any term t_r for CFSA in TD.

Likewise, EE in PD for CFSA can be expressed as follows. where $\sigma^{\mathrm{PD}}_{\mathrm{CFSA},O}$ denotes the countrywide aggregate capacity of all MNOs O at any term t_r for CFSA in PD. Also, $P_{\mathrm{SC,m},o,l,s} = P_{\mathrm{m}}$ denotes the maximum transmission power of an SBS s of MNO o in a building l.

4) SESA WITHOUT APPLYING THE FRAMEWORK

If the proposed framework is not applied (i.e., without applying the spectrum trading, spectrum sharing, and spectrum reusing mechanisms) to SESA, the allocated spectrum M to each MNO o in the primary-level is scheduled to its small cell UEs in a building orthogonally both in time and frequency without changing the transmission power of any SBS. This results in the same average capacity, SE, and EE in TD, FD, and PD of any MNO o in a country. Hence, the system-level average capacity, SE, and EE of all MNOs O at any term t_r in SESA without applying the framework (SESAW) in either TD, FD, or PD can be given as follows.

$$\sigma_{\mathrm{SESAW},O} = \sum_{o=1}^{O}\left(\begin{array}{l}\sigma_o^{\mathrm{MC}} \\ +\sum_{l=1}^{L}\left(\sum_{s=1}^{S_{\mathrm{F},l}}\sum_{t\in T}\sum_{i=1}^{M}\sigma_{o,l,s,t,i}\left(\rho_{o,l,s,t,i}\right)\right)\end{array}\right) \tag{44}$$

$$\gamma_{\mathrm{SESAW},O} = \sigma_{\mathrm{SESAW},O}\Big/\left(\left(M_{\mathrm{C}}+\sum_{o=1}^{O}M_o^{\mathrm{MC}}\right)\times Q\right) \tag{45}$$

$$\varepsilon_{\mathrm{SESAW},O} = \frac{\sum_{o=1}^{o}\left(\begin{array}{c}\sum_{l=1}^{L}\left(\sum_{s=1}^{S_{\mathrm{E},l}}P_{\mathrm{SC,m},o,l,s}\right) \\ +\left(S_{\mathrm{P},o}\times P_{\mathrm{PC}}\right)+\left(S_{\mathrm{M},o}\times P_{\mathrm{MC}}\right)\end{array}\right)}{\left(\sigma_{\mathrm{SESAW},O}/Q\right)} \tag{46}$$

5) PERFORMANCE IMPROVEMENT FACTOR

We consider SESAW as the reference technique to show the outperformance in terms of the average capacity, SE, and EE of SESA, FUSA, and CFSA techniques. For example, the average capacity, SE, and EE outperformance of SESA in TD over that of SESAW can be expressed by the following performance improvement factors.

$$\zeta^{\mathrm{TD}}_{\mathrm{SESA},O} = \sigma^{\mathrm{TD}}_{\mathrm{SESA},O}\Big/\sigma_{\mathrm{SESAW},O} \tag{47}$$

$$\xi^{\mathrm{TD}}_{\mathrm{SESA},O} = \gamma^{\mathrm{TD}}_{\mathrm{SESA},O}\Big/\gamma_{\mathrm{SESAW},O} \tag{48}$$

$$\varsigma^{\mathrm{TD}}_{\mathrm{SESA},O} = \varepsilon^{\mathrm{TD}}_{\mathrm{SESA},O}\Big/\varepsilon_{\mathrm{SESAW},O} \tag{49}$$

Like (47)-(49), the average capacity, SE, and EE outperformance of SESA, FUSA, and CFSA techniques over that of SESAW technique in any domain can be derived. Note that the improvement factor for the average capacity, SE, and EE is directly affected by the intra-building reuse factor ω_l. For example, using (33) and (44), it can be found that $\zeta^{\mathrm{TD}}_{\mathrm{SESA},O}$ improves directly by ω_l(i.e., intra-building reuse factor). Hence, by changing the value of ω_l, the average capacity improvement $\zeta^{\mathrm{TD}}_{\mathrm{SESA},O}$ can be changed.

IV. PERFORMANCE EVALUATION

A. DEFAULT PARAMETERS AND ASSUMPTIONS

In addition to Table 5, the detailed simulation parameters and assumptions used to evaluate the system-level performances can be found in [40], [44], which are in line with the recommendations from the standardization bodies. BS transmission power and coverage, channel model, antenna gain and pattern, UE speed, and TTI are considered for the 3GPP E-UTRA simulation case 3 [40], [44], [47]. Further, though there exists a number of high-frequency bands for 5G and beyond systems, we consider the 28 GHz bands as it has already been adopted in practical 5G networks in several countries [48]. Furthermore, each multistory building consists of 6 floors, each having 8 apartments. An SBS (a Closed Subscriber Group femtocell) of each MNO is considered to be deployed in each apartment and serves one of its UEs at a time. Due to a balance in fairness and throughput performances, we consider one frequency-domain proportional fair (PF) scheduler per 3D cluster of SBSs such that RBs of the mmWave spectrum bandwidth are scheduled to all

$$\varepsilon^{\mathrm{PD,hy}}_{\mathrm{SESA},\,O} = \frac{\sum_{o=1}^{o}\left(\begin{array}{c}\sum_{l=1}^{L}\left(\omega_l\times\sum_{s=1}^{S_{\mathrm{3D},l}}\left(\begin{array}{c}P_{\mathrm{SC,m},o,l,s} \\ +\left(\begin{array}{c}\left(\left(2^{O-1}-1\right)/2^{O-1}\right) \\ \times\left(P_{\mathrm{SC,iw},o,l,s}+P_{\mathrm{SC,ul},o,l,s}\right)\end{array}\right)\end{array}\right)\right) \\ +\left(S_{\mathrm{P},o}\times P_{\mathrm{PC}}\right)+\left(S_{\mathrm{M},o}\times P_{\mathrm{MC}}\right)\end{array}\right)}{\left(\sigma^{\mathrm{PD,hy}}_{\mathrm{SESA},O}/Q\right)} \tag{41}$$

TABLE 5. Default parameters and assumptions.

Parameters and Assumptions		Value
Countrywide spectrum bandwidth[7]	28 GHz	200 MHz
	2 GHz	40 MHz
Total number of MNOs[7] and subscribers[7]		4 and N_C, respectively
Number of subscribers for MNOs 1, 2, 3, and 4 respectively[7]	SESA	25%, 25%, 25%, and 25% of N_C
	FUSA	40%, 30%, 20%, and 10% of N_C
	CFSA	100%, 100%, 100%, and 100% of N_C
Maximum power of an SBS (interweave)	P_m	19 dBm
Reduced power scaling factors (underlay)	α_1	30%
	α_2	15%
	α_3	10%
Interference threshold (underlay)	I_m	$0.3P_m$
per MNO		
Cellular layout[2]		Hexagonal grid, dense urban, 3 sectors per macrocell site
Transmission direction		Downlink
Number of MBSs and PBSs		1 and 2
Antenna configuration		Single-input single-output (all BSs and UEs)
Number of UEs	Macrocell	30
	Picocell	4 (offloaded)
	Small cell	$L\times 48$
Number of buildings and picocell coverage		L and 40 m (radius)
PF scheduler time constant (t_c) and t_r		100 ms and 6 months
Total simulation run time		8 ms

taken [2]from [49] and form [7][6].

SBSs within each 3D cluster of a building by the respective frequency-domain PF scheduler based on the channel condition of each SBS-UE link. Moreover, the full buffer traffic model is considered such that an SBS can be assumed to have user traffic to serve in each TTI during the simulation run time. Finally, the performance results are generated by a simulator built using the computational tool MATLAB R2012b in a personal computer by repeating the simulation experiment eight times, which uses the default parameters and assumptions detailed above and shown in Table 5.

Remark 3: We assume one frequency-domain PF scheduler for all SBSs per building and an SBS usually covers a small area such that only a few numbers of UEs can be served by an SBS at a time. Moreover, a PF scheduler typically checks the current channel conditions of UEs to allocate RBs in the system bandwidth to them such that as long as there exists a single UE in the system, the scheduler

$$\varepsilon_{\mathrm{CFSA},O}^{\mathrm{TD}}=\frac{\sum_{o=1}^{o}\left(\sum_{l=1}^{L}\left(\omega_l\times\sum_{s=1}^{S_{3\mathrm{D},l}}\sum_{k=0}^{(|\boldsymbol{O}|-1)}\left(\begin{pmatrix}O-1\\k\end{pmatrix}\times\left(P_{\mathrm{SC,m},o,l,s}/2^{O-1}\right)\right)\right)+\left(S_{\mathrm{P},o}\times P_{\mathrm{PC}}\right)+\left(S_{\mathrm{M},o}\times P_{\mathrm{MC}}\right)\right)}{\left(\sigma_{\mathrm{CFSA},O}^{\mathrm{TD}}/Q\right)}\tag{42}$$

$$\varepsilon_{\mathrm{CFSA},O}^{\mathrm{PD}}=\frac{\sum_{o=1}^{o}\left(\sum_{l=1}^{L}\left(\omega_l\times\sum_{s=1}^{S_{3\mathrm{D},l}}\left(\left(P_{\mathrm{SC,m},o,l,s}/2^{O-1}\right)+\sum_{k=1}^{(|\boldsymbol{o}|-1)}\left(\begin{pmatrix}O-1\\k\end{pmatrix}\times\left(\left(\alpha_k\times P_{\mathrm{SC,m},o,l,s}\right)/2^{o-1}\right)\right)\right)\right)+\left(S_{\mathrm{P},o}\times P_{\mathrm{PC}}\right)+\left(S_{\mathrm{M},o}\times P_{\mathrm{MC}}\right)\right)}{\left(\sigma_{\mathrm{CFSA},O}^{\mathrm{PD}}/Q\right)}\tag{43}$$

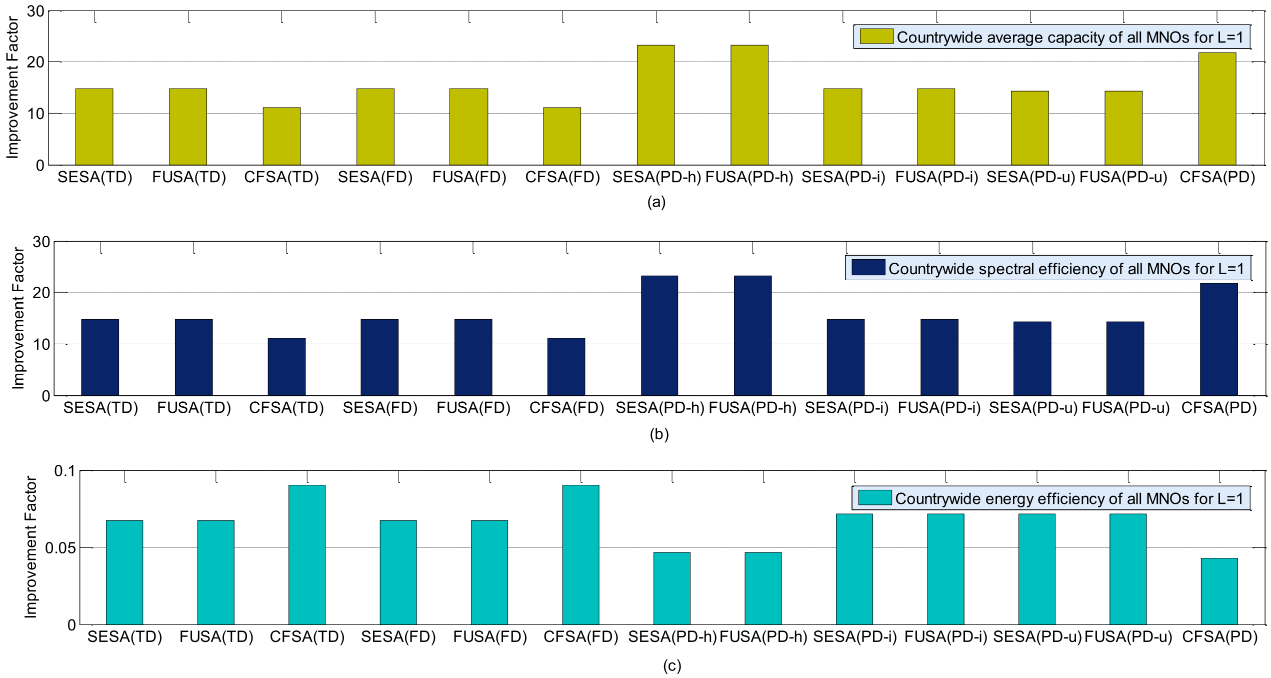

FIGURE 7. Average capacity, SE, and EE performance improvement factors for all techniques in each domain with respect to that of SESAW for $L = 1$ for $\omega = 6$.

TABLE 6. The minimum value of L (L_{MIN}) to satisfy the prospective SE and EE requirements for 6G mobile systems.

RF	L																$L_{\min}$
	TD				FD				PD								
	SESA/ FUSA		CFSA		SESA/ FUSA		CFSA		SESA/ FUSA						CFSA		
									Hybrid		Interweave		Underlay				
	SE	EE	SE	EE	SE	EE	SE	EE	SE	EE	SE	EE	SE	EE	SE	EE	
1	13	1	17	1	13	1	17	1	9	1	13	1	14	1	9	1	9
6	3	1	3	1	3	1	3	1	2	1	3	1	3	1	2	1	2
12	2	1	2	1	2	1	2	1	1	1	2	1	2	1	1	1	1

can allocate the whole system bandwidth at any TTI. Furthermore, the indoor channel condition of a high-frequency line-of-sight (LOS) signal changes insignificantly within a short distance due to the low speed of a UE. Because of these reasons, for a given system bandwidth, there is an insignificant impact on the overall system-level capacity, SE, and EE from the multi-user diversity gain, particularly for a few numbers of UEs served over a small coverage area by an SBS.

Moreover, if there is a change (e.g., an increase) in the number of UEs of any SBS (e.g., SBS x) at any TTI, the PF scheduler may schedule some of the RBs allocated already to UEs of other SBSs within a building back to the new UEs of SBS x. This, however, does not affect the overall aggregate capacity of MNO o noticeably since RBs are simply rescheduled from one SBS to another due to the change in the number of UEs of each SBS over time for a given system bandwidth. Due to such an insignificant impact on the overall performances, even though the proposed framework can be investigated for the case of multiple UEs served simultaneously by each small cell of an MNO, such an issue is not taken into account to keep the overall analysis simple. Hence, for the purpose of simplicity and finding closed-form solutions, following other existing literature [15], [32], [41]–[43], we also assume that an SBS can serve one UE at a time.

B. PERFORMANCE RESULTS

1) SINGLE BUILDING OF SBSS

We consider a single building of SBSs to present the basic trends in the average capacity, SE, and EE performances of SESA, FUSA, and CFSA techniques in TD, FD, and PD with respect to that of SESAW, which are explained in detail for multiple buildings of SBSs (i.e., $L > 1$) later. Figure 7 shows the average capacity, SE and, EE performances of all techniques in each domain with respect to that of SESAW for a single building of SBSs (i.e., $L = 1$) with intra-building RF $\omega = 6$. As presented earlier mathematically, it can be found that the average capacity, SE, and EE responses in TD, FD, and PD for SESA and FUSA (also presented as SESA/FUSA) are the same as shown in Fig.7.

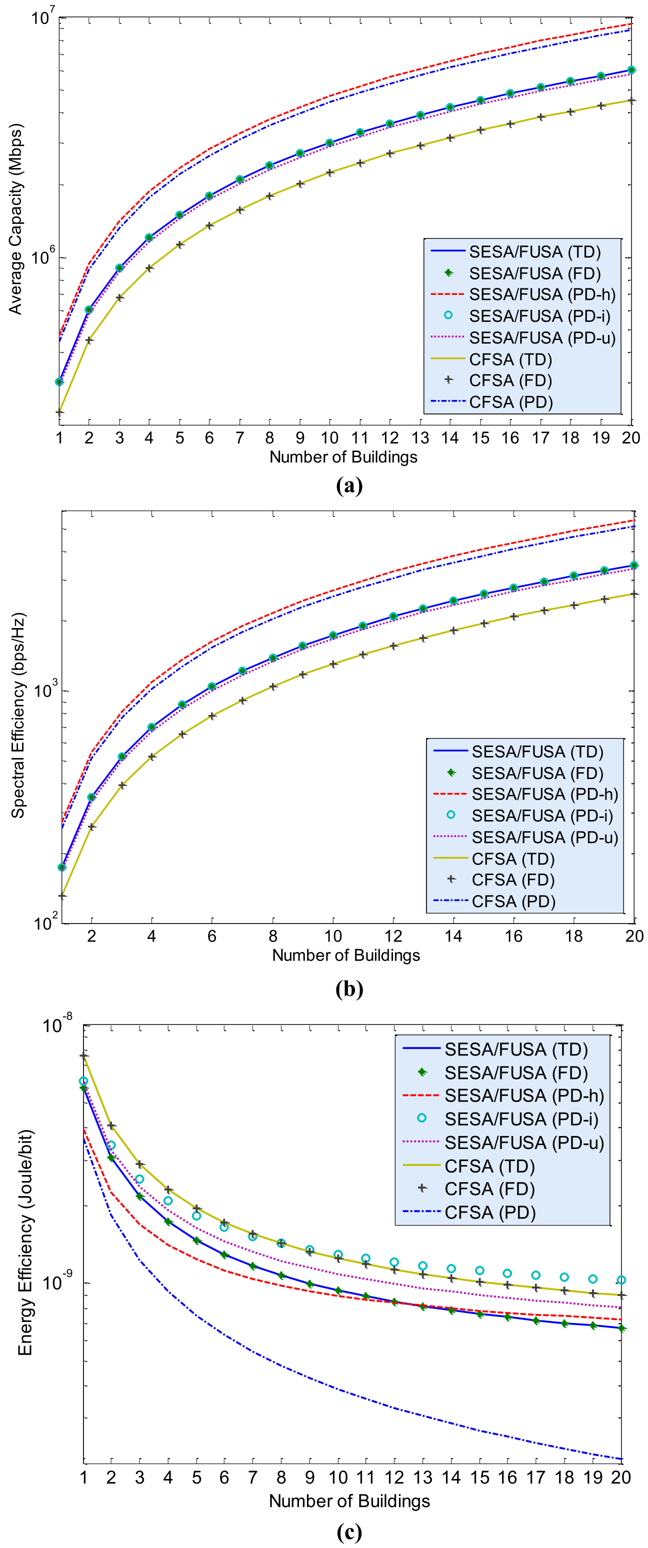

FIGURE 8. Average capacity, SE and, EE performances for all techniques in each domain for $\omega = 6$ with the variation in the number of buildings of SBSs (i.e., $L > 1$).

Moreover, for $L = 1$, it can be found from Fig.7 that in both TD and FD (also termed as TD/FD), the average capacity and SE improve significantly by about 15 times in SESA/FUSA, whereas about 11 times in CFSA, over that in SESAW. Since the EE is inversely related to the achievable capacity, the EE improves as well considerably by reducing the energy required per bit transmission to only 6.75% in SESA/FUSA and about 9% in CFSA in comparison with that in SESAW.

However, the average capacity, SE, and, EE performances in PD outperform even further than that in TD/FD in all techniques. More specifically, in PD, the average capacity and SE improve by about 15 times in SESA/FUSA (when employing either the interweave spectrum access or the underlay spectrum access) and about 22 times in CFSA, over that in SESAW. These correspond to a reduction in the energy required per bit transmission to about 7.1% in SESA/FUSA and about 4.3% in CFSA as compared to that in SESAW in PD.

Note that, the performances of SESA/FUSA in PD can be improved further by employing both the interweave and the underlay spectrum access techniques. For example, an improvement in the average capacity and SE by about 23 times, as well as a reduction in the energy required per bit transmission to about 4.6%, can be achieved in PD by employing the hybrid interweave-underlay spectrum access technique to SESA/FUSA. These, however, cause to increase in the overall cost and complexity due to implementing both the interweave and underlay spectrum access techniques in SESA/FUSA.

Overall, SESA, FUSA, and CFSA techniques outperform considerably in terms of the average capacity, SE and, EE in TD, FD, and PD over that in SESAW, and PD provides the best performances in the average capacity, SE and EE in all techniques.

2) MULTIPLE BUILDINGS OF SBSS

a: TD/FD PERFORMANCES

Like Fig.7, in TD/FD, SESA/FUSA provides relatively better capacity and SE performances than that of CFSA for $L > 1$. This is because, in TD/FD, an SBS of any MNO o in SESA/FUSA can operate at the licensed spectrum of its own MNO o in addition to that of the shared spectra licensed by other MNOs $\boldsymbol{O}\backslash o$. In contrast, an SBS in CFSA can operate only at a portion of the countrywide full spectrum in TD/FD, the amount of which varies depending on the existence of the number of interferer small cell UEs of other MNOs $\boldsymbol{O}\backslash o$ in each TTI t. Moreover, in SUSA/FUSA, since an SBS of an MNO o has multiple transceivers (each operating at the allocated spectrum in the primary-level to an MNO), an idle transceiver of the SBS over a number of TTIs can be switched off if there is no request from its users' traffic to be served, resulting in reducing the energy consumption of SUSA/FUSA in TD/FD.

Contrary to that, in TD/FD CFSA, an SBS operates only at a single transceiver on the countrywide full spectrum such that the transceiver needs to be switched on in all TTIs even when serving relatively low traffic volume. This results in the lower EE performance of CFSA than that of SESA/FUSA in

TABLE 7. A list of notations.

Notation	Description
t, i, and *l*	Index of a transmission time interval, a resource block, and a building, respectively
T	Simulation run time
O	Maximum number of MNOs of a country
o	Index of an MNO
M	Amount of mmWave spectrum per MNO in SESA
L	Number of buildings per macrocell
P_{MC}, P_{PC}, and P_{SC}	The transmission power of a macrocell, a picocell, and a small cell, respectively
k	The number of interferer UEs for a small cell of an MNO o in an apartment
P_m and P_r	The maximum transmission power and the reduced transmission power of an SBS of MNO o
$\alpha_1, \alpha_2, \cdots, \alpha_{\lvert o\rvert-1}$	Scaler quantities each representing a percentage of the total transmission power of an SBS
I_m	CCI threshold when small cells operate under the underlay spectrum access
$\zeta^{TD}_{SESA,O}$, $\xi^{TD}_{SESA,O}$, and $\varsigma^{TD}_{SESA,O}$	Average capacity, SE, and EE outperformance of SESA in TD over that of SESAW
M_C	Countrywide 28 GHz mmWave spectrum in resource blocks
t_r	Spectrum renewal term
M_o	Amount of licensed spectrum in resource blocks of any MNO o
M_o^{MC} and N_o^{MC}	Macrocell spectrum in resource blocks and macrocell UEs of an MNO o
N_o and N_C	Number of subscribers of an MNO o and a country, respectively
$S_{F,l}$	Number of SBSs in any building l
$S_{M,o}$	Number of macrocell base stations of an MNO o
$S_{P,o}$	Number of picocell base stations per macrocell base station of an MNO o
ω_l	Spectrum RF for MNO o in building l
ω_{MC}	Spectrum RF for a macrocell of MNO o
ω	Spectrum RF for each MNO in each building
I_a^{thr} and I_e^{thr}	Intra-floor and inter-floor CCI constraints at a small cell UE
Ξ_a and Ξ_e	The maximum number of co-channel small cells in the intra-floor level and inter-floor level of an MNO o
Δ_m	The minimum distance between a co-channel small cell and a small cell UE
s_l^a and s_l^e	The number of small cells corresponding to $\Delta_{a,l}$ and $\Delta_{e,l}$, respectively
α_f Δ_e	Floor penetration loss at the 28 GHz mmWave spectrum corresponding to Δ_e
Δ_a and Δ_e	A minimum distance between co-channel small cells for the 28 GHz mmWave spectrum in the intra-floor level and inter-floor level, respectively, for MNO o at any term t_r
$S_{3D,l}$	Number of small cells per 3D cluster in a building l
σ_o^{MC}	The average capacity of all macrocell UEs of MNO o

TABLE 7. *(Continued.)* A list of notations.

$\sigma^{TD}_{SESA,O}$, $\sigma^{TD}_{FUSA,O}$, and $\sigma^{TD}_{CFSA,O}$	The countrywide system-level average capacity of all MNOs O at any term t_r for SESA, FUSA, and CFSA in TD, respectively
$\gamma^{TD}_{SESA,O}$, $\gamma^{TD}_{FUSA,O}$, and $\gamma^{TD}_{CFSA,O}$	System-level average SE in SESA, FUSA, and CFSA techniques in TD
$\varepsilon^{PD,hy}_{SESA,O}$	Average EE in Joules/bit in PD (for the hybrid interweave-underlay spectrum access) in SESA (and FUSA)
$\varepsilon^{TD}_{CFSA,O}$	EE in TD (and FD) in CFSA

TD/FD. Hence, for $L > 1$, CFSA outperforms SESA/FUSA (when operating either at the interweave or at the underlay spectrum access technique) in PD, whereas, SESA/FUSA outperforms CFSA in TD/FD, in terms of average capacity, SE, and EE performances. Note that both the average capacity and SE improve linearly, whereas the EE improves negative-exponentially, as intra-building RF ω and inter-building RF L increase irrespective of SESA, FUSA, and CFSA techniques operating either in TD/ FD or in PD as shown in Fig.8.

b: PD PERFORMANCES

Figure 8 shows the average capacity, SE, and EE performances of all techniques in each domain with the variation in the number of buildings of SBSs, L. Like Fig.7 for $L = 1$, with the variation of L in PD, CFSA outperforms in terms of the average capacity, SE, and EE over that in SESA/FUSA when employing either the interweave spectrum access or the underlay spectrum access. However, when employing the hybrid interweave-underlay spectrum access technique to SESA/FUSA in PD, SESA/FUSA can provide somewhat better performances in the average capacity, SE, and EE than that in CFSA. This can be clarified by the fact that in PD, an SBS of an MNO o can get access to the full countrywide spectrum in each TTI in CFSA in contrast to sharing a portion of the full spectrum allocated in level 1 to any of the interferers MNOs $\boldsymbol{O}\backslash o$. This results in an SBS, even operating at a reduced transmission power of 10% to 30% of P_m in CFSA as compared to that of 30% of P_m in SESA/FUSA, achieving higher capacity and SE performances in CFSA than in SESA/FUSA. In PD, since an SBS in CFSA operates at a lower transmission power on average than in SESA/FUSA, CFSA also provides better EE performance than that of SESA/FUSA in PD.

C. PERFORMANCE COMPARISON

According to [1], [50]–[53], the future 6G mobile system is expected to provide SE of 370 bps/Hz and EE of 0.3 uJ/bit. Table 6 shows the minimum values of the inter-building RF L required by SESA, FUSA, and CFSA techniques operating in TD, FD, as well as PD, to satisfy the aforementioned prospective SE and EE requirements for 6G mobile systems. It can be found from Table 6 that all techniques operating in any domain can achieve the prospective SE and EE requirements for the 6G mobile system. Note that for each technique, the lower the value of the RF in the intra-building level, the higher the value of the RF in the inter-floor level (i.e., the value of L) is required to satisfy the prospective SE and EE requirements for 6G. In other words, the product of the intra-building RF and the inter-building RF defines the total number of times the same countrywide full spectrum can be reused to SBSs such that by varying either the intra-building RF or the inter-building RF, the prospective SE and EE requirements for 6G can be satisfied.

Since the SE and EE performances of any technique in one domain vary from another, a technique and its operating domain requiring the minimum value of L can be defined. In this regard, for an intra-building RF of 12, CFSA, as well as SESA/FUSA (when employing the hybrid interweave-underlay spectrum access technique), in PD can achieve the prospective SE and EE requirements for 6G by reusing the countrywide full spectrum to the minimum number of buildings of SBSs (i.e., $L = 1$) as shown in Table 6. However, when employing either the interweave or the underlay spectrum access technique to the PD SESA/FUSA, the CFSA in PD outperforms (in terms of L) all other techniques operating in any domain to achieve the prospective SE and EE requirements for 6G mobile systems.

V. CONCLUSION

In this paper, we have given a broad overview on how to improve mmWave spectrum utilization for 5G and beyond systems by means of presenting a framework concerning the improvement of the utilization of the 28 GHz mmWave spectrum allocated to MNOs in a country using numerous spectrum allocation techniques of SESA, FUSA, and CFSA. Various spectrum utilization improvement mechanisms such as spectrum trading, spectrum sharing, and spectrum reusing have been exploited into SESA, FUSA, and CFSA spectrum allocation techniques in major four domains, including time, frequency, power, and space, using indoor small cells in a multi-operator network scenario. Orthogonal allocation of TTIs and RBs to small cells subject to the CCI constraint in time-domain (TD) and frequency-domain (FD), respectively, whereas controlling the transmission power of small cells and reusing the same allocated spectrum of any MNO more than once within each building of small cells in power-domain (PD) and space-domain (SD), respectively, have been considered.

Using the Equal Likelihood Criterion and the properties of left-justified Pascal's triangle, we have derived the system-level average capacity, spectral efficiency (SE), and energy efficiency (EE) performance metrics for SESA, FUSA, and CFSA techniques in each domain. Extensive system-level numerical and simulation results and analyses have been carried out to evaluate the performance of SESA, FUSA, and CFSA in TD, FD, PD, and SD for an arbitrary country with four MNOs. It has been found that a change in either the inter-building RF L or an intra-building RF ω changes the performance improvement such that the product of L and ω defines the degree of performance improvement in average capacity, SE, and EE for each spectrum allocation technique in any domain. Moreover, irrespective of the values of L and ω, CFSA outperforms SESA/FUSA (when operating either at the interweave or at the underlay spectrum access technique) in PD, whereas, SESA/FUSA outperforms CFSA in TD/FD, in terms of average capacity, SE, and EE performances. Finally, it has been shown that all techniques operating in any domain can achieve the prospective SE and EE requirements for the 6G mobile system. Additionally, CFSA, as well as SESA/FUSA (when employing the hybrid interweave-underlay spectrum access technique), in PD can achieve the prospective SE and EE requirements for 6G mobile systems by reusing the countrywide full spectrum to the minimum number of buildings of small cells.

APPENDIX

See Table 7.

REFERENCES

[1] S. Chen, Y.-C. Liang, S. Sun, S. Kang, W. Cheng, and M. Peng, "Vision, requirements, and technology trend of 6G: How to tackle the challenges of system coverage, capacity, user data-rate and movement speed," *IEEE Wireless Commun.*, vol. 27, no. 2, pp. 218–228, Apr. 2020.

[2] S. J. Kim, E. C. Kim, S. Park, and J. Y. Kim, "Dynamic spectrum allocation with variable bandwidth for cognitive radio systems," in *Proc. 9th Int. Symp. Commun. Inf. Technol.*, Sep. 2009, pp. 106–109.

[3] I. F. Akyildiz, W.-Y. Lee, M. C. Vuran, and S. Mohanty, "NeXt generation/dynamic spectrum access/cognitive radio wireless networks: A survey," *Comput. Netw.*, vol. 50, no. 13, pp. 2127–2159, Sep. 2006.

[4] R. K. Saha, "Evolution toward spectrum utilization-centric network: Addressing high capacity with limited spectrum bandwidth," in *Proc. Panel: Adv. Commun. Technol. (SoftNet)*, Porto, Portugal, Oct. 2020, pp. 18–28. [Online]. Available: http://www.iaria.org/conferences2020/filesICSNC20/Communications Technologies_Panel.pdf

[5] R. K. Saha, "On evaluating spectrum allocation techniques in millimeter-wave systems using indoor smalls for 5G/6G," in *Proc. 15th Int. Conf. Syst. Netw. Commun. (ICSNC)*, Porto, Portugal, Oct. 2020, pp. 28–31.

[6] R. K. Saha, "On exploiting millimeter-wave spectrum trading in countrywide mobile network operators for high spectral and energy efficiencies in 5G/6G era," *Sensors*, vol. 20, no. 12, p. 3495, Jun. 2020.

[7] R. K. Saha, "Licensed countrywide full-spectrum allocation: A new paradigm for millimeter-wave mobile systems in 5G/6G era," *IEEE Access*, vol. 8, pp. 166612–166629, 2020.

[8] X. Yan, Q. Song, H. Zhang, and L. Shao, "Dynamic spectrum allocation based on cognitive radio," in *Proc. 5th Asia–Pacific Conf. Environ. Electromagn.*, Sep. 2009, pp. 254–257.

[9] Z. Wei, D. Yang, and L. Sang, "Dynamic system level frequency spectrum allocation scheme based on cognitive radio technology," *China Commun.*, vol. 11, no. 7, pp. 84–91, Jul. 2014.

[10] J. Gu, "Dynamic spectrum allocation algorithm for resolving channel conflict in cognitive vehicular networks," in *Proc. 7th IEEE Int. Conf. Electron. Inf. Emergency Commun. (ICEIEC)*, Macau, China, Jul. 2017, pp. 413–416.

[11] R. K. Saha, "Underlay cognitive radio millimeter-wave spectrum access for in-building dense small cells in multi-operator environments toward 6G," in *Proc. 23rd Int. Symp. Wireless Pers. Multimedia Commun. (WPMC)*, Oct. 2020, pp. 105–110.

[12] R. Kumer Saha, "Interweave shared-use model for dynamic spectrum access in millimeter-wave mobile systems for 6G," in *Proc. IEEE 92nd Veh. Technol. Conf. (VTC-Fall)*, Nov. 2020, pp. 1–6.

[13] R. K. Saha, "A flexible licensed spectrum allocation technique for millimeter-wave mobile systems toward 6G," in *Proc. 23rd Int. Symp. Wireless Pers. Multimedia Commun. (WPMC)*, Oct. 2020, pp. 117–122.

[14] R. K. Saha, "Approaches to improve millimeter-wave spectrum utilization using indoor small cells in multi-operator environments toward 6G," *IEEE Access*, vol. 8, pp. 207643–207658, 2020.
[15] R. K. Saha, "A new paradigm for spectrum allocation in millimeter-wave systems," in *Proc. 15th Int. Conf. Syst. Netw. Commun. (ICSNC)*, Porto, Portugal, Oct. 2020, pp. 14–17.
[16] R. K. Saha, "A massive millimeter-wave spectrum allocation and exploitation technique toward 6G mobile networks," in *Proc. 15th Int. Conf. Syst. Netw. Commun. (ICSNC)*, Porto, Portugal, Oct. 2020, pp. 32–41.
[17] M. L. Attiah, A. A. M. Isa, Z. Zakaria, M. K. Abdulhameed, M. K. Mohsen, and I. Ali, "A survey of mmWave user association mechanisms and spectrum sharing approaches: An overview, open issues and challenges, future research trends," *Wireless Netw.*, vol. 26, no. 4, pp. 2487–2514, May 2020.
[18] M. Rebato, F. Boccardi, M. Mezzavilla, S. Rangan, and M. Zorzi, "Hybrid spectrum sharing in mmWave cellular networks," *IEEE Trans. Cognit. Commun. Netw.*, vol. 3, no. 2, pp. 155–168, Jun. 2017.
[19] H. Kamal, M. Coupechoux, and P. Godlewski, "Inter-operator spectrum sharing for cellular networks using game theory," in *Proc. IEEE 20th Int. Symp. Pers., Indoor Mobile Radio Commun.*, Tokyo, Japan, Sep. 2009, pp. 425–429.
[20] S. K. Joshi, K. B. S. Manosha, M. Codreanu, and M. Latva-aho, "Dynamic inter-operator spectrum sharing via Lyapunov optimization," *IEEE Trans. Wireless Commun.*, vol. 16, no. 10, pp. 6365–6381, Oct. 2017.
[21] R. K. Saha, "A dynamic exclusive-use spectrum access method for millimeter-wave mobile systems toward 6G," in *Proc. IEEE 92nd Veh. Technol. Conf. (VTC-Fall)*, Victoria, BC, Canada, Nov. 2020, pp. 1–6.
[22] F. Hu, B. Chen, J. Wang, M. Li, P. Li, and M. Pan, "MastDP: Matching based double auction mechanism for spectrum trading with differential privacy," in *Proc. IEEE Global Commun. Conf. (GLOBECOM)*, Waikoloa Village, HI, USA, Dec. 2019, pp. 1–6.
[23] M. K. Farshbafan, M. H. Bahonar, and F. Khaiehraveni, "Spectrum trading for Device-to-Device communication in cellular networks using incomplete information bandwidth-auction game," in *Proc. 27th Iranian Conf. Electr. Eng. (ICEE)*, Yazd, Iran, Apr. 2019, pp. 1441–1447.
[24] D. Niyato, E. Hossain, and Z. Han, "Dynamics of multiple-seller and multiple-buyer spectrum trading in cognitive radio networks: A game theoretic modeling approach," *IEEE Trans. Mobile Comput.*, vol. 8, no. 8, pp. 1009–1022, 2009.
[25] Z. Hu, Z. Zheng, L. Song, T. Wang, and X. Li, "UAV offloading: Spectrum trading contract design for UAV-assisted cellular networks," *IEEE Trans. Wireless Commun.*, vol. 17, no. 9, pp. 6093–6107, Sep. 2018.
[26] N. Saquib, E. Hossain, and D. Kim, "Fractional frequency reuse for interference management in LTE-advanced hetnets," *IEEE Wireless Commun.*, vol. 20, no. 2, pp. 113–122, Apr. 2013.
[27] P. Yen, Q. Zhan, and H. Minn, "New fractional frequency reuse patterns for multi-cell systems in time-varying channels," *IEEE Wireless Commun. Lett.*, vol. 4, no. 3, pp. 253–256, Jun. 2015.
[28] R. A. Hassan, A. Idris, H. Adto, M. Ramadhan, and M. Kassim, "Reduction of inter-cell interference in close proximity cell using dynamic fractional frequency reuse method," in *Proc. IEEE Conf. Syst., Process Control (ICSPC)*, Malacca, Malaysia, Dec. 2017, pp. 157–161.
[29] R. K. Saha and C. Aswakul, "A tractable analytical model for interference characterization and minimum distance enforcement to reuse resources in three-dimensional in-building dense small cell networks," *Int. J. Commun. Syst.*, vol. 30, no. 11, p. e3240, Jul. 2017.
[30] R. Kumer Saha, "Modeling interference to reuse millimeter-wave spectrum to in-building small cells toward 6G," in *Proc. IEEE 92nd Veh. Technol. Conf. (VTC-Fall)*, Nov. 2020, pp. 1–6.
[31] R. K. Saha, "Spectrum sharing in satellite-mobile multisystem using 3D in-building small cells for high spectral and energy efficiencies in 5G and beyond era," *IEEE Access*, vol. 7, pp. 43846–43868, 2019.
[32] R. K. Saha, "A technique for massive spectrum sharing with ultra-dense in-building small cells in 5G era," in *Proc. IEEE 90th Veh. Technol. Conf. (VTC-Fall)*, Honolulu, HI, USA, Sep. 2019, pp. 1–7.
[33] R. K. Saha, "A countrywide licensed full spectrum allocation method for millimeter-wave mobile systems for 6G," in *Proc. IEEE 92nd Veh. Technol. Conf. (VTC-Fall)*, Nov. 2020, pp. 1–7.
[34] R. K. Saha, "Hybrid interweave-underlay millimeter-wave spectrum access in multi-operator cognitive radio networks toward 6G," in *Proc. 15th Int. Conf. Syst. Netw. Commun. (ICSNC), Porto, Portugal, Oct.*, vol. 2020, pp. 42–48.
[35] R. K. Saha, "A theoretical framework toward realizing spectral and energy efficiencies of 6G mobile networks," in *Proc. IEEE 92nd Veh. Technol. Conf. (VTC-Fall)*, Nov. 2020, pp. 1–7.
[36] R. K. Saha, "On maximizing energy and spectral efficiencies using small cells in 5G and beyond networks," *Sensors*, vol. 20, no. 6, p. 1676, Mar. 2020.
[37] *5G Wikipedia*. Accessed: Feb. 28, 2021. [Online]. Available: https://en.wikipedia.org/wiki/5G
[38] R. H. Tehrani, S. Vahid, D. Triantafyllopoulou, H. Lee, and K. Moessner, "Licensed spectrum sharing schemes for mobile operators: A survey and outlook," *IEEE Commun. Surveys Tuts.*, vol. 18, no. 4, pp. 2591–2623, 4th Quart., 2016.
[39] *Definition of Spectrum Use and Efficiency of a Radio System (Question ITU-R 47/1)*, document Recommendation ITU-R SM.1046-1, 1994-1997. Accessed: Jan. 12, 2021. [Online]. Available: https://www.itu.int/dms_pubrec/itu-r/rec/sm/R-REC-SM.1046-1-199710-S!!PDF-E.pdf
[40] R. K. Saha, "Dynamic allocation and sharing of millimeter-wave spectrum with indoor small cells in multi-operator environments toward 6G," *EURASIP J. Wireless Commun. Netw. (JWCN)*, vol. 2020, pp. 1–16, Dec. 2020.
[41] D. Chen, T. Jiang, and Z. Zhang, "Frequency partitioning methods to mitigate cross-tier interference in two-tier femtocell networks," *IEEE Trans. Veh. Technol.*, vol. 64, no. 5, pp. 1793–1805, May 2015.
[42] R. K. Saha, "A hybrid system and technique for sharing multiple spectrums of satellite plus mobile systems with indoor small cells in 5G and beyond era," *IEEE Access*, vol. 7, pp. 77569–77596, 2019.
[43] R. K. Saha, S. Nanba, and K. Nishimura, "A technique for cloud based clustering and spatial resource reuse and scheduling of 3D in-building small cells using CoMP for high capacity CRAN," *IEEE Access*, vol. 6, pp. 71602–71621, 2018.
[44] R. K. Saha, "A hybrid interweave–underlay countrywide millimeter-wave spectrum access and reuse technique for CR indoor small cells in 5G/6G era," *Sensors*, vol. 20, no. 14, p. 3979, 2020.
[45] *Pascal's Triangle*. Accessed: Oct. 19, 2020. [Online]. Available: https://en.wikipedia.org/wiki/Pascal%27s_triangle
[46] R. K. Saha, "3D spatial reuse of Multi-Millimeter-Wave spectra by ultra-dense in-building small cells for spectral and energy efficiencies of future 6G mobile networks," *Energies*, vol. 13, no. 7, p. 1748, Apr. 2020.
[47] *Evolved Universal Terrestrial Radio Access (E-UTRA); Radio Frequency (RF) System Scenarios*, document 3GPP TR 36.942, V.1.2.0, 3rd Generation Partnership Project, Jul. 2007. Accessed: Feb. 15, 2020. [Online]. Available: https://portal.3gpp.org/ desktopmodules /Specifications/SpecificationDetails.aspx?specificationId=2592
[48] *Japan Assigns 5G Spectrum to four Operators-5G Observatory*. 5G Observatory. Accessed: Apr. 22, 2020. [Online]. Available: https://5gobservatory.eu/japan-assigns-5g-spectrum-to-four-operators/
[49] *Simulation Assumptions and Parameters for FDD HeNB RF Requirements*. document 3GPP, TSG RAN WG4 (Radio) Meeting #51, R4-092042, May 2009. Accessed: Feb. 13, 2020. [Online]. Available: https://www.3gpp.org/ftp/tsg_ran/WG4_Radio/TSGR4_51/Documents/
[50] Z. Zhang, Y. Xiao, Z. Ma, M. Xiao, Z. Ding, X. Lei, G. K. Karagiannidis, and P. Fan, "6G wireless networks: Vision, requirements, architecture, and key technologies," *IEEE Veh. Technol. Mag.*, vol. 14, no. 3, pp. 28–41, Sep. 2019.
[51] C.-X. Wang, F. Haider, X. Gao, X.-H. You, Y. Yang, D. Yuan, H. Aggoune, H. Haas, S. Fletcher, and E. Hepsaydir, "Cellular architecture and key technologies for 5G wireless communication networks," *IEEE Commun. Mag.*, vol. 52, no. 2, pp. 122–130, Feb. 2014.
[52] R. K. Saha, "Dynamic spectrum sharing in multi-operator millimeter-wave indoor systems," in *Proc. 20th Int. Conf. Netw. (ICN)*, Porto, Portugal, Apr. 2021, pp. 1–2.
[53] G. Auer, V. Giannini, C. Desset, I. Godor, P. Skillermark, M. Olsson, M. Imran, D. Sabella, M. Gonzalez, O. Blume, and A. Fehske, "How much energy is needed to run a wireless network?" *IEEE Wireless Commun.*, vol. 18, no. 5, pp. 40–49, Oct. 2011.

RONY KUMER SAHA received the B.Sc. degree in electrical and electronic engineering from the Khulna University of Engineering and Technology (KUET), in 2004, the M.Eng. degree in information and communications technologies from the Asian Institute of Technology (AIT), Thailand, in 2011, and the Ph.D. degree in electrical engineering from Chulalongkorn University, Thailand, in 2017.

He worked as a Lecturer and later promoted to an Assistant Professor with American International University-Bangladesh (AIUB), Bangladesh, from January 2005 to August 2013. From September 2013 to July 2014, he was with East West University, Bangladesh. Since 2017, he has been working as a Research Engineer with the Radio and Spectrum Laboratory, KDDI Research, Inc., Japan. He has research experiences on mobile wireless communications in universities and industries for more than ten years. He has authored about 60 peer-reviewed, reputed, and highly recognized international journals (such as IEEE Access, *International Journal of Communication Systems* (Wiley), *Mobile Information Systems* (Hindawi), *Wireless Communications and Mobile Computing* (Wiley/Hindawi), *Sensors* (MDPI), *Energies* (MDPI), and *IEEJ Transactions on Electrical and Electronic Engineering* (Wiley) and conferences (IEEE ICC, IEEE GLOBECOM, IEEE PIMRC, IEEE VTC, IEEE DySPAN, WPMC, ICSNC, ICN, and ECTI-CON) papers. He also filed an international patent. His current research interests include 5G and beyond ultra-dense HetNets, spectrum sharing, policy, and management in multiple communication systems, and millimeter-wave communications.

Dr. Saha served as a member of the Fronthaul Working Group, xRAN Forum, USA, a TPC Member of the 2018 IEEE Global Communications Conference Workshops and the 2021 IARIA ICNS, and a Steering Committee Member of IARIA ICSNC 2021. He also served as the Session Chair for two sessions, namely Radio Resource Management and Aerial Networks at the 2019 IEEE VTC-Fall, Honolulu, HI, USA, and the 2019 IEEE International Symposium on Dynamic Spectrum Access Networks Newark, NJ, USA, for the session Spectrum Sharing in 5G, and a Reviewer for a number of recognized journals, including IEEE Transactions on Vehicular Technology, *IEEE Wireless Communications*, IEEE Access, *Physical Communication* (Elsevier), *International Journal of Communication Systems* (Wiley), *Sensors* Journal (MDPI), *Symmetry* Journal (MDPI), *Mobile Information Systems* (Hindawi), and *Sustainability* Journal (MDPI). Since 2019, he has been serving as an Associate Editor of the *Engineering Journal*, Thailand.